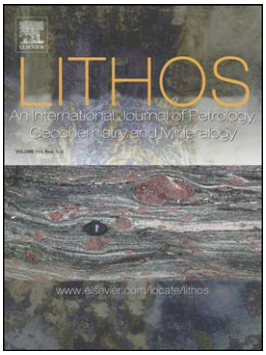

Ancient xenocrystic zircon in young volcanic rocks of the southern Lesser Antilles island arc

Yamirka Rojas-Agramonte, Ian Williams, Richard Arculus, Alfred Kröner, Antonio García-Casco, Concepción Lázaro, Stephan Buhre, Jean Wong, Helen Geng, Carlos Morales Echeverría, Teresa Jeffries, Hangqian Xie, Regina Mertz-Kraus

PII: S0024-4937(17)30272-4
DOI: doi:10.1016/j.lithos.2017.08.002
Reference: LITHOS 4385

To appear in: *LITHOS*

Received date: 10 March 2017
Accepted date: 7 August 2017

Please cite this article as: Rojas-Agramonte, Yamirka, Williams, Ian, Arculus, Richard, Kröner, Alfred, García-Casco, Antonio, Lázaro, Concepción, Buhre, Stephan, Wong, Jean, Geng, Helen, Echeverría, Carlos Morales, Jeffries, Teresa, Xie, Hangqian, Mertz-Kraus, Regina, Ancient xenocrystic zircon in young volcanic rocks of the southern Lesser Antilles island arc, *LITHOS* (2017), doi:10.1016/j.lithos.2017.08.002

Ancient xenocrystic zircon in young volcanic rocks of the southern Lesser Antilles island arc

Yamirka Rojas-Agramonte[1,2,3], Ian Williams[4]; Richard Arculus[4], Alfred Kröner[1,2]; Antonio García-Casco[5,6]; Concepción Lázaro[5], Stephan Buhre[1], Jean Wong[7], Helen Geng[7], Carlos Morales Echeverría[8], Teresa Jeffries [9]; Hangqian Xie[2], Regina Mertz-Kraus[2]

[1]Beijing SHRIMP Center, Chinese Academy of Geological Sciences, 26 Baiwanzhuang Road, 100037 Beijing, China

[2]Institut für Geowissenschaften, Johannes Gutenberg-Universität, Becherweg 21 D-55099 Mainz, Germany

[3]Departamento de Geociencias, Universidad de los Andes, Cra 1 No 18A – 70, M1-309, Bogota, Colombia

[4]Research School of Earth Sciences, Australian National University, Canberra, ACT 2601, Australia

[5]Departamento de Mineralogía y Petrología, Universidad de Granada, Fuentenueva s/n, 18071 Granada, Spain.

[6]Instituto Andaluz de Ciencias de la Tierra, CSIC-Universidad de Granada, 18100 Armilla, Granada. Spain.

[7]Department of Earth Sciences, The University of Hong Kong, Pokfulam Road, Hong Kong, China.

[8]Centro de Investigaciones del Petróleo (CEINPET) Washington No169 esq. a Churruca, 12000 Cerro, Ciudad de la Habana

[9]Science Facilities department, Imaging and Analysis Center, Natural History Museum, Cromwell Road, London, SW7 5BD

ABSTRACT

The Lesser Antilles arc is one of the best global examples in which to examine the effects of the involvement of subducted sediment and crustal assimilation in the generation of arc crust. Most of the zircon recovered in our study of igneous and volcaniclastic rocks from Grenada and Carriacou (part of the Grenadines chain) is younger than 2 Ma. Within some late Paleogene to Neogene (~34–0.2 Ma) lavas and volcaniclastic sediments however, there are Paleozoic to Paleoarchean (~250–3469 Ma) xenocrysts, and late Jurassic to Precambrian zircon (~158–2667 Ma) is found in beach and river sands. The trace element characteristics of

zircon clearly differentiate between different types of magma generated in the southern Lesser Antilles through time. The zircon population from the younger arc (Miocene, ~22–19 Ma, to Present) has minor negative Eu anomalies, well-defined positive Ce anomalies, and a marked enrichment in heavy rare earth elements (HREE), consistent with crystallization from very oxidized magmas in which Eu^{2+} was in low abundance. In contrast, zircon from the older arc (Eocene to mid-Oligocene, ~30–28 Ma) has two different REE patterns: 1) slight enrichment in the light (L)REE, small to absent Ce anomalies, and negative Eu anomalies and 2) enriched High (H)REE, positive Ce anomalies and negative Eu anomalies (a similar pattern is observed in the xenocrystic zircon population). The combination of positive Ce and negative Eu anomalies in the zircon population of the older arc indicates crystallization from magmas that were variably, but considerably less oxidized than those of the younger arc. All the igneous zircon has positive εHf(t), reflecting derivation from a predominantly juvenile mantle source. However, the εHf(t) values vary significantly within samples, reflecting considerable Hf isotopic heterogeneity in the source.

The presence of xenocrystic zircon in the southern Lesser Antilles is evidence for the assimilation of intra-arc crustal sediments and/or the recycling and incorporation of sediments into the magma sources in the mantle wedge. Most likely however, primitive magmas stalling and fractionating during their ascent through the Antilles crust entrained ancient zircon. This is evidence by the geochemistry of the study samples, which is inconsistent with any involvement of partially melted detrital Proterozoic and younger subducted sediment. Paleogeographic reconstructions show that the old zircon could derive from distant regions such as the Eastern Andean Cordillera of Colombia, the Merida Andes, and the northern Venezuela coastal ranges, transported for example by the Proto-Maracaibo River precursor of the Orinoco River.

Keywords: Lesser Antilles, island arc, crustal assimilation, Grenada, Carriacou, Petite Martinique, zircon, xenocryst, U-Pb dating, ^{230}Th disequilibrium, Hf isotopes, rare earth elements, Ce and Eu anomalies

1. Introduction

The main source of global volcanic arc magmas is the peridotitic “wedge” of mantle between a subducted slab and overriding lithosphere (Arculus, 1994). The wedge also contains fluid-soluble components from the subducted slab where rising magmas generated in this heterogeneous wedge may assimilate or partially melt and mingle with overriding

lithosphere. The various components are potentially identifiable by means of their trace element and isotopic characteristics (Hofmann, 1988; Condie, 2005; Pearce, 2008; Mann and Schmidt, 2015), but the processes responsible for the mixing of sources and transfer of material are complex. They involve several mechanisms including: a) reactive bulk assimilation (e.g., Beard et al., 2005); b) physical transport of fractionated fluids and melts liberated from the deep mantle as well as subducted slab components that infiltrate the mantle along grain boundaries, fractures, and diapirs (Spandler and Pirard, 2013); and c), infiltrating diapirs of subduction mélanges that eventually melt at the slab-mantle interface or within the infiltrated mantle below the arc (Gerya and Yuen 2003; King et al., 2006; Castro and Gerya 2008; Castro et al., 2010; Behn et al., 2011; Marschall and Schumacher, 2012).

Subduction plays a major role in recycling oceanic and continental crust into the mantle, including sediments formed after erosion of continental material, and also accounts for the development of chemical heterogeneities in the upper mantle (Hofmann and White, 1982). The occurrence of old zircon in juvenile intra-oceanic arc rocks raises the questions of how much recycled crust contributed to these rocks and how old continent- and/or mantle-derived zircon grains became entrained in volcanic arc rocks (Rojas-Agramonte et al., 2016). Zircon from subducted continental and oceanic sources might become entrained in the mantle above a subduction zone and ultimately be transferred to a volcanic arc in supra-subduction mantle-derived melts, providing physical evidence for the recycling process (Rojas-Agramonte et al., 2016). On the other hand, crustal relamination (Hacker et al., 2011), assimilation of sediments embedded in oceanic arc-crust (Bezard et al., 2014) and subduction erosion of fore-arcs (Stern, 2011) or ancient basement of continental margins (Scholl and von Huene, 2009) might also potentially account for such occurrences.

The Lesser Antilles arc (Fig.1a) is one of the best global examples where phenomena associated with the subduction of sediments and assimilation of overriding crust can be studied. The arc is recognized as having the most "continental crust-like" geochemical and isotopic characteristics of all modern island arcs (Chauvel et al., 2012), and features a wide range of magmatic compositions (Macdonald et al., 2000). Debate continues regarding the effects of intra-crustal assimilation-fractional crystallization (e.g., Bezard et al., 2015) versus inputs of subducted sediment (Carpentier et al., 2008). The southernmost islands (e.g. Grenada, Carriacou, and Petite Martinique; Figs. 1 and 2) are notable for their abnormally radiogenic Sr and Pb isotopic compositions, consistent with the involvement of recycled continental crust-derived and subducted sediment (Carpentier et al., 2008; Labanieh et al., 2010, O'Neill, 2016) and/or high-level crustal assimilation through AFC processes (Thirlwall

et al., 1996). These islands provide an opportunity to compare and contrast the effects of sediment involvement in the generation of arc crust by means of subduction versus intra-crustal recycling.

The Orinoco River (Fig. 1b), which drains the northern part of the South American continent (i.e., Andes to the west, northern Venezuela coastal ranges, and the Precambrian Guyana Shield), is the main source of terrigenous sediment with highly radiogenic Pb that contributes to the trench and fore-arc basin fill of the southern Lesser Antillean arc (Westbrook et al., 1984). Our U-Pb dating of zircon from the arc magmas shows for the first time the presence of Late Jurassic to Precambrian zircon, which provides compelling evidence for assimilation of sedimentary intra-arc crust and/or recycling and incorporation of sediments into the magma sources in the mantle wedge. The results of this study also better constrain the age and composition of the different volcanic associations on Grenada, Carriacou, and Petite Martinique.

1.1 The Lesser Antilles intra-oceanic arc

The Lesser Antilles island arc (Fig. 1a) represents the eastern expression of a relatively long-lived arc-system (Bouysse et al., 1990; Macdonald et al., 2000) that began its evolution in the eastern Paleo-Pacific Ocean during the Early Cretaceous (Bouysse 1984; Pindell et al., 2005). The current arc is Cenozoic (Eocene to present) in age and developed in response to westward subduction of Atlantic oceanic lithosphere beneath the leading edge of the Caribbean plate at ~ 18–20 mm a^{-1} (de Mets et al., 2000; Weber et al., 2001). This rate is slow compared to other island arcs worldwide where convergence rates can be up to 20 cm a^{-1} (Bird, 2003) and potentially could have led to higher than normal temperatures in the subducted slab (at a given depth), causing partial melting of the subducted sediments (Macdonald et al., 2000; Turner et al., 2016).

Several studies have highlighted marked changes in elemental and isotopic compositions along-strike of the arc. These are probably the result in part of the changing age and composition of the subducting material in front of the arc system (Carpentier et al., 2008, 2009). According to Bezard et al. (2015), two main processes have been proposed to explain this extreme compositional variation: (1) incorporation of subducted sediment into the mantle source; or (2), significant assimilation of sediment-rich arc crust. Both processes could of course be involved. A high sediment input to the source could be explained by the presence of abundant sediment in the southern Antilles Trench due to discharge mostly from the Orinoco and Amazon Rivers (e.g., Carpentier et al., 2008, 2009).

The nature of the basement of the Southern Lesser Antilles arc (from St. Vincent to Grenada) remains poorly known. Bouysse et al. (1990) suggested that the volcanic arc is underlain by a basement composed of Mesozoic volcanic arc rocks known as the proto-arc. Alternatively, according to Aitken et al. (2011), the central-southern Lesser Antilles arc developed above a deep fore-arc basin of the (now extinct) Aves Ridge arc, splitting it into the Grenada and Tobago basins (Fig. 1a). South of Martinique (Fig. 1a), rocks of the Cenozoic arc show the imbrication of older and younger arcs (Bouysse et al., 1984; Macdonald et al., 2000; Germa et al., 2011). The older arc was active from the beginning of the early Eocene to the mid-Oligocene (30–28 Ma), whereas the younger arc has been active since the early Burdigalian (22–19 Ma) (Germa et al., 2011).

The sediment-derived fluid contribution to the mantle source in the southern islands is most likely related to subduction of clastic sediments building up the large Barbados accretionary prism (Turner et al., 1996; Carpentier et al., 2008; 2009). The southern fore-arc region (Barbados Ridge; Fig. 1) constitutes a thick and extensive accretionary complex consisting of more than 10 km of sediments with a large proportion of terrigenous turbidites and U-rich black shales. The sediments have very radiogenic Pb isotope ratios and unradiogenic Nd and Hf isotopic compositions, implying a much larger component of old continental material than other oceanic sediments worldwide (Vervoort et al., 2011). Such features can be attributed to the overwhelming contribution of detrital material derived from an old (heterogeneous) continental source such as the Guyana Shield and Amazon Craton (Fig. 1b; Carpentier et al., 2008).

2. Geological background

Grenada, Carriacou and Petite Martinique comprise *inter alia* the nation of Grenada and are located at the southern end of the Lesser Antilles (Figs. 1 and 2). Grenada is the largest of these islands (Fig. 2).

2.1. Grenada

The main island of Grenada has an area of 312 km^2 (Fig. 2), rising to a maximum height of 840m. One characteristic geological feature of the island is the large surface area of secondary or reworked volcanic material, caused by erosion of primary volcanic deposits (Arculus, 1976). The oldest rocks on the island belong to the Tufton Hall Formation that comprises tectonically disturbed and well-bedded sequences of calcareous shale, siltstone and sandstone containing foraminifera dated as upper Eocene to lower Oligocene (Saunders et al., 1985). Tuffaceous horizons and limestones are interbedded with these lithologies. The presence of

exotic volcanic lithic fragments of andesitic or basaltic composition and abundant plagioclase and pyroxene mineral grains, as well as tuffaceous horizons, indicates that igneous activity already occurred in the Eocene (Arculus, 1973). The pyroxene grains are very fresh suggesting penecontemporaneous volcanic activity (Saunders et al., 1985) which corresponds to the activity of the older Lesser Antilles arc (Arculus, 1973).

Miocene to Recent volcanic rocks were erupted from several centers which overlie the Paleogene sedimentary basement of the Tufton Hall Formation. These volcanic rocks include basanitoids, alkalic (strongly silica-undersaturated) and subalkalic basalts, andesites and dacites (Arculus, 1976; 1978; Devine, 1987; 1995, Thirlwall et al., 1996; Stamper et al., 2014). The mineralogy and petrology of the Grenada volcanic rocks represent an unusual combination of alkalic and calc-alkaline (cf. Arculus, 2004) features with abundant highly magnesian and silica-undersaturated basalts. Two distinct basaltic series have been identified: the M-series for microphyric basalts and the C-Series for ankaramitic basalts (Thirlwall and Graham 1984). The low Sr M-series (basalt-andesite-dacite suite) is characterized by MgO contents higher than 10 wt.% in the mafic parental magmas, and by its olivine–microphyric character. The M-series contains ultramafic xenoliths included in alkali basalt, and these are among the rare global occurrences of peridotite in island arcs (Parkinson et al., 2003). Associated with the M-series basalts is a chemically contiguous suite of high-SiO_2 basalts and basaltic andesites whose compositions converge with the evolved products of the C-series (Thirlwall et al., 1996; Stamper et al., 2014).

The C-series is characterized by parental high-Sr, ankaramitic basalt, with higher CaO abundances at any given MgO content than any other volcanic suite in the arc, and is strongly clinopyroxene–phyric (see Schiano et al., 2000 for review). These rocks have more radiogenic Nd and less radiogenic Sr and Pb than the M-series (Hawkesworth et al., 1979). Differentiation of C-series basalts also produced andesites and dacites (Thirlwall et al. 1996). The compositional variation within the C-series is dominated by fractional crystallization of augite and plagioclase (Thirlwall and Graham 1984).

The absolute age of the rocks in Grenada is not well known and is based on only a limited number of K-Ar and ^{39}Ar-^{40}Ar analyses (Geotermica Italiana, 1981; Speed et al., 1993 and summarized in Robertson, 2005 with source data from Briden et al., 1979). The oldest reported age of 21.2±1.0 Ma comes from an andesite dome at Mt Craven north of the island (Fig. 2; Briden et al., 1979) whereas the youngest age (1.6±1.4 Ma) comes from a dacite north of Gouyave (Fig. 2).

2.2. Carriacou and Petite Martinique

Carriacou, with a surface area of c. 32 km^2 and elevations of up to 290 m, is located 30 km north of Grenada (Fig. 2). The island is composed of a succession of volcanic and sedimentary rocks that range in age from Eocene to Pleistocene (Jackson et al., 2008; Donovan et al., 2003; 2013). The oldest rocks on Carriacou (based on paleontological evidence) are late Eocene to early Oligocene in age and include the Belvedere (sample GR45) and Anse la Roche formations and the Cherry Hill and Bogles units (Speed et al., 1993; Donovan et al., 2003). The Belvedere and Anse la Roche formations are synchronous in part and have a similar range of lithologies: well-bedded interstratified pelagic and turbiditic volcanogenic rocks. The two units are juxtaposed by the Bogles thrust (Speed et al., 1993).

Miocene volcanic and sedimentary rocks are more widespread on the island and are separated from the Paleogene succession by an angular unconformity (Jackson et al., 2008; Donovan et al., 2003). The predominantly subaerial volcanism during this period produced mainly pyroclastic deposits containing ejected plutonic blocks, with minor lava flows, dome lavas and dykes. Briden et al. (1979) reported whole-rock K-Ar ages ranging from 18.1 to 2.87 Ma for these rocks.

The volcanic rocks have been divided into six units based on differences in their phenocryst assemblages (Caldwell et al., 1984). Their composition ranges from basalt through basaltic andesite to andesite with island arc tholeiitic affinity and minor occurrences of calc-alkaline rocks (Jackson et al., 2008; Caldwell et al., 1984). The chemical composition of the basaltic rocks is similar to that of M- and C-series basalts in Grenada (Arculus 1976; Jackson 1980). Contemporaneous volcanic-derived sedimentary rocks are also present on the island, the Grand Bay Formation (sample GR42) being the youngest Miocene unit (Fig. 2). The Grand Bay Formation consists mainly of volcanic-derived conglomerate, sandstone and siltstone. Microphyric basalt dykes intruded the older sedimentary and volcanic sequences during the late Miocene. These dykes appear to have originated from centers located in Petite Martinique, ~ 4 km east of Carriacou (Fig. 2), and Saline, ~1.5 km to the south. The geology and stratigraphy of Carriacou has been described in detail by Caldwell et al. (1984), Jackson et al. (2008) and Donovan et al. (2003; 2013).

Petite Martinique has a surface area of 2.37 km^2. It is dominated by a 230 m summit in the center, formerly part of a volcanic cone. Apart from the geochemistry of one sample (WPM255) reported by Jackson (1980), little is known about the geology of the island. Photos of the collected rock types are included in the Supplementary Material A (Fig. SM 1).

3. Methodology

3.1.Samples analyzed

Grenada, Carriacou, and Petite Martinique were sampled systematically for lithologies ranging from basalt to dacite and volcanic-derived sedimentary rocks. In addition, sand samples were collected and panned locally for heavy minerals in riverbeds and on beaches (Tables S1 and S2 of the Supplementary Material). The use of sand samples derived from volcanic rocks avoids potential contamination from rock-crushing equipment. Eleven sand samples were obtained from Grenada and three from Carriacou. Of the zircon grains recovered from sands, more than 300 were analyzed (Table S3). We employed the panning technique in addition to whole-rock sampling to ensure that xenocristic zircon found in the rocks was also present in sand samples, excluding laboratory contamination as its source. Similar techniques have been applied successfully in Mauritius (Torsvik et al., 2013) and Indonesia (Sevastianova et al., 2011).

Fifty-three samples were collected on the three islands. In the following list, the underlined and bold labels correspond to sediments and volcanic-derived sediments. Twelve samples from Grenada (GR1, GR5, **GR6**, **GR7**, GR12, GR13, GR14, GR15, GR16, GR23, GR24, **GR30**), two from Carriacou (**GR42**, **GR45**), and two from Petite Martinique (PM2a, 2b) contain zircon (see Table S1 and Fig. 2 for description and sample location). In the main text below we focus on, and describe, the rocks containing zircon, although information on the location and composition of the remaining samples is summarized in Supplementary Tables S4 and S5.

3.2.Analytical methods

Rock samples about 1 to 2 kg in weight were crushed to a grain size of ~ 250 μm using a jaw crusher and roller mill. A heavy mineral fraction was then produced by panning with water and using a Frantz magnetic separator. The final heavy mineral concentrate (mostly zircon and apatite) was obtained by panning with water and alcohol in the Beijing SHRIMP Center, China. About 100 g of the homogenized coarse material from each of the 12 zircon-bearing igneous samples from Grenada and Petite Martinique (no igneous sample from Carriacou contained zircon) were powdered in a Siebtechnik tungsten carbide mill for chemical and whole-rock isotopic analysis. Whole-rock major and trace element concentrations were determined by X-ray fluorescence spectrometry (XRF) on fused glass beads and pressed powder pellets and by laser ablation-inductively coupled plasma-mass spectrometry (LA-ICP-MS) in the Institute for Geosciences, University of Mainz. Whole-rock

Rb-Sr and Sm-Nd isotopic analysis were carried out at the CIC (Centro de Instrumentación Científica) of the University of Granada, Spain.

The analytical techniques are described in detail in the Supplementary Material B. In summary, the zircon grains were analyzed using secondary ion mass spectrometry (SIMS) and LA-ICP-MS. The SIMS measurements were conducted on SHRIMP II instruments at the Beijing SHRIMP Center and the Research School of Earth Sciences, Australian National University. All samples younger than 2 Ma (GR5, GR12, GR14, GR15, GR16, GR24) were dated using the SHRIMP II in both Beijing and Canberra. The dates measured on both instruments were very similar, but the Canberra data were more precise because a much higher primary beam intensity and larger spot size were used, yielding higher count rates.

The zircon analytical data are summarized in Tables 1–4 and are plotted on concordia diagrams in Figs. 3-5. U-Pb dates were also measured by LA-ICP-MS at the Institute of Geosciences, University of Mainz, and the Natural History Museum, London. Hf-in-zircon isotope compositions and REE abundances were measured *in situ*, mostly on dated grains, at the LA-ICP-MS facility at Mainz University, and at the MC-LA-ICP-MS laboratory in the Department of Earth Sciences, The University of Hong Kong, China, respectively. U-Pb dating and trace element analyses of the detrital zircon grains recovered from beach and river sands were conducted simultaneously by LA-ICP-MS at the Institute of Geology and Geophysics, Chinese Academy of Sciences, Beijing, China.

3.3. U-Pb dating of zircon grains younger than 2 Ma: corrections for U-series disequilibrium and initial ^{230}Th.

It takes more than 2 Ma for the ^{238}U decay chain to reach isotopic equilibrium, so any dates based on the measured ^{206}Pb/^{238}U in zircon of that age or younger must be corrected for U-series disequilibrium. Corrections are also required for initial ^{230}Th, a parent isotope of ^{206}Pb present in all Th-bearing minerals. A simple procedure for correcting measured Pb/U dates for initial ^{230}Th was proposed by Schärer (1984). The relative amount of disequilibrium ^{230}Th was defined by the degree of Th-U fractionation between mineral and magma as a factor *f*, where $f = (\mathrm{Th/U})_{\mathrm{mineral}} / (\mathrm{Th/U})_{\mathrm{melt}}$. The relationship between the measured ^{206}Pb/^{238}U and age (t) is thereby:

$$^{206}\mathrm{Pb}/^{238}\mathrm{U} = (e^{\lambda_{238}t} - 1) + \lambda_{238}/\lambda_{230} * (f - 1)$$

A more rigorous relationship that takes into account the ingrowth of ^{230}Th was proposed by von Quadt et al. (2014), based on the work of Sakata et al. (2013).

$$^{206}Pb/^{238}U = (e^{\lambda_{238}t} - 1) + \lambda_{238}/\lambda_{230} * (f - 1) * (1 - e^{-\lambda_{230}t}) * e^{\lambda_{238}t}$$

As good as these approximations are, neither takes into account disequilibrium in the other relatively long-lived intermediate daughter products in the ^{238}U decay chain, namely ^{234}U ($t_{½}$ = 245.6 ka) and ^{226}Ra ($t_{½}$ = 1.6 ka). For very young samples, such as those included in the present study, both have a significant effect in slowing the ingrowth of radiogenic ^{206}Pb, leading to a potential underestimation of ages calculated from $^{206}Pb/^{238}U$.

For the present work, the effects of U-series disequilibrium were calculated from first principles using the equations of Bateman (1910). In doing so it was assumed that the U incorporated into the zircon was in ^{238}U-series equilibrium and that the Th/U of the melt from which the zircon crystallized was the same as the Th/U of the host rock, a reasonable assumption given the high melt fraction that would have been present in the erupted magmas. For detrital zircon, the melt Th/U was assumed to be the average Th/U of all analyzed rock samples from Grenada. The Th-U fractionation between mineral and magma (*f*) was calculated separately for each analyzed spot before the correction for initial ^{230}Th and U-series disequilibrium was applied. The results were then compared with those given by the correction procedures recommended by Schärer (1984) and von Quadt et al. (2014). Broadly speaking, for a normal zircon Th/U of 0.5, the three methods were in close agreement for dates > 800 ka. For ages <800 ka, the Schärer (1984) result became increasingly divergent from the other two, and only below 300 ka did the von Quadt et al. (2014) result and ours deviate by more than 1%, a measure of the accuracy of the von Quadt et al. (2014) approximation.

4. Results

The petrology, mineralogy, as well as whole-rock and isotope geochemistry of Grenada lavas have been extensively described by Arculus (1973, 1976, 1978), Shimizu and Arculus (1975), Hawkesworth et al. (1979), Thirlwall and Graham (1984), Devine (1987, 1995), Stamper et al. (2014) and O'Neill (2016), whereas there are more limited data for Carriacou by Jackson (1980), Caldwell et al. (1984) and Caldwell (1983). There are no published petrological-geochemical data for rocks from Petite Martinique.

4.1. Whole rock geochemistry

4.1.1. Major and trace elements (Grenada and Petite Martinique)

Most of the dated lavas contain 54–60 wt.% SiO_2, 0.39–0.90 wt.% TiO_2, 16–18 wt.% Al_2O_3 and of 1.3–11 wt.% MgO (Grenada) and 13 wt.% MgO (Petit Martinique) (Table S6). The sample compositions partly overlap the IUGS alkaline-subalkaline discriminant boundary (Le Bas et al., 1986), but most can be classified as subalkaline/tholeiitic dacite (GR13, PM2a), andesite (GR1, GR5, GR6), tuffogenic basalt (GR6), trachy-andesite (PM2b), basaltic andesite (GR12, GR14, GR15, GR23, GR24), and basalt (GR16) (Fig. 6). The chondrite-normalized ($_N$) REE patterns are similar for all samples and are characterized by slight enrichment in the light rare earth elements (LREE). $(La/Yb)_N$ ranges from 2 to 17 with higher $(La/Yb)_N$ in samples from Petite Martinique (PM2a, PM2b, 30–46). The REE patterns are characterized by the absence of Eu anomalies (Eu/Eu* = 0.9–1.1; Figs. 7a, c, e; Table S6). The absence of a negative Eu anomaly, despite abundant evidence for fractionation of plagioclase in the genesis of evolved magmas from basaltic parents on Grenada, indicates crystallization under highly oxidizing conditions with an absence of Eu^{2+} (see also Stamper et al., 2014, and discussion below of chondrite-normalized REE abundance patterns for zircon).

Primitive mantle-normalized multi-element plots show an enrichment in slab-derived elements such as Th, variably in Pb and Sr relative to the LREE, and negative concentration anomalies in the high-field strength elements (HFSE) Nb and Ti (Figs. 7b, d, f). Some samples have a small negative Ce anomaly. In general, these chemical characteristics are consistent with melting of subduction-modified mantle involving fluids and/or melts from a dehydrating slab (Münker et al., 2004). A melted sedimentary component (Johnson and Plank, 1999) in these samples is suggested by the Th/Nb ratios ranging from 0.44 to 2.16 (Table S6) when compared to a ratio of ~ 0.05 in basalt derived from the depleted asthenospheric mantle (Hofmann, 1988). In addition, the Th/Yb vs Ba/La plot (not shown) indicates that, with one single exception, the magmas from where our samples are derived contain a larger sediment component than most of the rocks from the Soufrière Volcanic Complex (SVC; Saint Lucia; Fig. 1a) studied by Bezard et al. (2015). This would indicate an even larger continental component containing fluid mobile elements which is not a feature expected if subducted sediments, from which fluid mobile elements had escaped, were the contaminant. On the other hand, high Ce/Pb ratios (12–74), except for three samples (5–9), are unlike most arc magmas (Ce/Pb ~ 4; Hofmann et al., 1986), indicative of muted development of positive Pb spikes in samples containing zircon (Fig. 7). Some samples however, display a negative Pb anomaly and correspond to samples that do not contain zircons (Fig. 7b)

4.1.2. Whole rock isotopic (Sm-Nd and Rb-Sr) systematics and model ages

Whole-rock Sm-Nd and Rb-Sr isotopic analyses were carried out at the University of Granada (Spain). The analytical procedures are described in Supplementary Material B. Sm-Nd and Rb-Sr concentrations as well as Nd isotopic compositions for 9 samples are listed in Table S7 together with the initial ε_{Nd}-values ($\varepsilon_{Nd(t)}$). The samples exhibit a narrow spectrum of $\varepsilon_{Nd(t)}$-values from +2.3 to +4.7 in rocks younger than ~ 5 Ma; sample GR6 from the Tufton Hall Formation (32 Ma) has an initial ε_{Nd}-value of -0.3. The samples have low $^{147}Sm/^{144}Nd$ (0.1093–0.1690), and initial $^{87}Sr/^{86}Sr$ ranges from 0.70555 to 0.70439 (Fig. 8). The Th/Nb ratios and LREE-patterns are consistent with variable proportions of recycled sediment in these samples, and the low initial $\varepsilon_{Nd(t)}$-values are consistent with involvement of terrigenous material (Carpentier et al., 2009). Curiously, the samples that contain old zircon (GR15, GR16 and GR23) have slightly higher whole-rock initial $\varepsilon_{Nd(t)}$ (3.95, 4.54 and 4.73, respectively) than similar samples without old zircon. We suggest that the Nd whole-rock isotopic system is not affected by old/inherited zircon because zircon contains virtually no Nd.

4.2. U–Pb zircon geochronology and cathodoluminescence images

Previous isotopic age measurements on rocks from Grenada, all by the K-Ar whole-rock method, have been summarized by Robertson (2005). The ages range from 0.98 ± 0.10 to 21.2 ± 1.0 Ma and are mainly from fresh olivine basalt, some andesites and two dacite samples. Multiple episodes of volcanism have been recognized in Grenada, Carriacou and Petit Martinique, so the presentation and discussion of zircon dates measured in the present study is divided by age range: ~ 0.2–1 Ma, ~4–6 Ma, ~12–16 Ma, ~30–34 Ma and zircon older than 40 Ma and xenocrysts (with dates ranging between 45.7 ± 1.6 and 3442 ± 42 Ma). Following the recommendations of Black and Jagodzinski (2003) all dates < 1100 Ma were calculated from $^{206}Pb/^{238}U$, whereas older dates were based on $^{207}Pb/^{206}Pb$. $^{207}Pb/^{206}Pb$ dates calculated from discordant analyses are minimum age estimates.

4.2.1. Very young magmatic zircon ages ~0.2–1 Ma (GR5, GR12, GR14, GR15, GR16, GR24, SAND1 to SAND14)

Most of the very young zircon grains are pink in color, elongate prismatic, with sharp or slightly rounded pyramidal terminations, but stubby grains also occur. The CL images (Fig. 9a and Supplementary Figures SM 2 to 15) are predominantly light to medium gray, suggesting relatively low-U contents. Zoning is ubiquitous and ranges from concentric, oscillatory, to striped or patchy. Some grains have an irregular distribution of dark and light

domains under CL, presumably due to recrystallization, and such domains were not analyzed. Some grains in basalt sample GR12 show broad sector zoning, possibly indicative of crystallization at high temperature (Fig. 9a).

For comparison and quality control all these samples were analyzed using the SHRIMP II instruments in both Beijing and Canberra. In both laboratories the results are very similar within errors. The youngest sample from the island comes from an andesitic lava flow near Mount St. Catherine (GR5; Fig. 2). Forty-eight zircon grains were analyzed (Tables 2 and 3) and yielded a mean $^{206}Pb/^{238}U$ crystallization age of 230 ± 4 ka (Fig. 3a; Canberra) and 245 ± 13 (Beijing). Samples GR14, GR15 and GR16 come from a nearby locality north of St. George's (Fig. 2). Analysis of 10 grains from sample GR14, 6 grains from sample GR15, and 16 grains from sample GR16 yielded similar mean ages in both laboratories of ~580, ~570 and ~560 ka respectively (Fig. 3b; Tables 2 and 3). Ten grains analyzed from sample GR24, collected near Mount Qua Qua (Fig. 2) also yielded a mean age of ~580 ka (Fig. 3b; Tables 2 and 3) which indicates that all these samples are part of the same episode of middle Pleistocene magmatism. The SHRIMP dates for 17 zircon grains from sample GR12, collected in the southeast of the island, yielded a mean age of ~1030 ka (Tables 2 and 3). In Carriacou only a few grains (11 out of 76) of those recovered from the three beach sands (SAND 8-10) are younger than 2 Ma (Table S3). In contrast, zircon with dates less than 2 Ma (217 out of 297; Table S3) predominates in Grenada.

4.2.2. Ages of ~4–6 Ma (GR1, GR13)

Dacite samples GR1 and GR13 from Grenada (Fig. 2) contain mostly short- to long-prismatic zircons, commonly with slightly rounded pyramidal terminations. The CL images reveal poorly to well-developed igneous zonation, mainly represented by concentric oscillatory zoning (Fig. 9b). Many grains have dark cores under CL with very low luminescence (high-U), surrounded by highly luminescent zones (low-U). In some grains this alternation is repeated several times. Some grains with irregular and patchy interiors, probably due to metamictization, were not analyzed. The SHRIMP $^{206}Pb/^{238}U$ analyses (Beijing laboratory) for seven zircon crystals analyzed from GR1 are concordant and give dates ranging from 4.53 ± 0.20 to 5.16 ± 0.27 Ma (Table 1a) with a weighted mean age of 4.92 ± 0.22 Ma (Fig. 3c). These are interpreted to record igneous crystallization at the time of lava formation.

Four grains analyzed from sample GR13 yielded concordant $^{206}Pb^{238}U$ dates between 4.13 ± 0.17 and 4.46 ± 0.18 Ma (Table 1a) with a weighted mean age of 4.24 ± 0.28 Ma (Fig. 3d),

close to the age of GR1 and interpreted to record the same volcanic event. A small number of zircon grains from sand samples SAND 1, 7 and 10 from Grenada (Fig. 2) also record this event (Table S3). These ages may correspond to previously reported K-Ar whole-rock ages of 3.56–3.77 Ma (Robertson, 2005).

4.2.3. Ages of ~12–16 Ma (PM2a, PM2b, GR42)

Ages in the range 12–16 Ma (Beijing and London laboratories) were only obtained for zircon from volcanic-derived sandstone sample GR42 (Carriacou, Fig. 2) and andesite samples PM2a and PM2b (Petite Martinique, Fig. 2). The zircon grains are euhedral and prismatic in shape with well-developed concentric oscillatory or banded zoning (Fig. 8c). Seven grains from sample PM2a produced well-grouped results with a weighted mean age of 12.8 ± 0.1 Ma (Table 1a, Fig. 3e). Sample PM2b was measured by using both the SHRIMP and LA-ICP-MS techniques (Fig. 3f, 4a). Six grains were analyzed by SHRIMP and provided consistent and concordant analyses giving a mean $^{206}Pb/^{238}U$ age of 12.7 ± 0.1 Ma (Table 1b) whereas concordant analyses from seven additional grains analyzed by LA-ICP-MS gave a mean age of 14.1 ± 0.1 Ma (Table 4). These results are significantly different from each other and may reflect incorrect common Pb correction in the ICP_MS analyses.

Four grains from Carriacou (GR42) yielded well grouped and concordant LA-ICP-MS dates of 15 ± 1 to 16 ± 1 Ma (Table 1b), provinding a weighted mean age of 15.57 ± 0.48 Ma (Fig. 4b). The presence of fossils in this sample (*Paleonummulites dius* (A), Nummulitidae, *Amphistegina angulate, Amphistegina* sp, *Planogypsina* sp (1 specimen), *Globigerina* spp and fragments of algae and sea urchins) indicate an early Miocene age for the unit, consistent with the zircon ages.

In view of the zircon morphology, CL images and the consistent ages, we interpret these data to reflect a volcanic event on Carriacou and Martinique that apparently contributed little zircon-bearing lava to Grenada, where it is only recorded by a few dates measured on sand-derived zircon in samples SAND 7 (10.8 ± 0.5 Ma), SAND 9 (12.4 ± 0.4 Ma), and SAND 10 (12.0 ± 0.4, 12.2 ± 0.2, 12.9 ± 0.3, and 12.7 ± 0.2 Ma) (Table 4). There is also a K-Ar age of 14.0 ± 0.4 Ma for an olivine basalt from Grenada (Richardson, 2005). It is most likely that these zircons reflect volcanism assigned to the Miocene Grand Bay Formation (Robinson and Jung, 1972).

4.2.4. Ages of ~27–34 Ma (GR6, GR7, GR45)

Zircon ages in the range 27–34 Ma (Beijing, London and Mainz laboratories) were obtained from a tuff and a volcanic-derived sandstone on Grenada (GR6 and GR7) and from a foraminiferal sandstone on Carriacou (GR45). The samples from Grenada were collected from the flank of Mount St. Catherine and belong to the Tufton Hall Formation, whereas the Carriacou sample comes from the Belvedere Formation. The zircon grains are predominantly long-prismatic, but stubby crystals also occur, and many grains have slightly rounded terminations. The CL images are similar to those from samples GR1 and 13, the zircon having concentric oscillatory zoning predominating, but banded zoning is also found (Fig. 8c). Grains with irregular zoning are rare and were not analyzed.

SHRIMP analysis of 5 grains from sample GR6 and 9 grains from sample GR7 yielded homogeneous groups of slightly different but concordant dates, ranging from 30.5 ± 1.1 to 32.2 ± 1.1 Ma, with a weighted mean age of 32.0 ± 0.5 Ma, in sample GR6 (Table 1, Fig. 4c) and from 33.0 ± 1.3 to 35.7 ± 1.4 Ma, with a weighted mean age of 34.3 ± 0.4 Ma in sample GR7 (Table 1, Fig. 4d). Three detrital grains measured by LA-ICP-MS (London) from sample GR45 yielded a mean age of 34.0 ± 0.6 Ma (Fig. 4e) suggesting derivation from a homogeneous source. Furthermore, thirteen detrital grains from sample GR45 measured by LA-ICP-MS at Mainz University yield dates ranging from 26.9 ± 1.1 to 34.4 ± 1.7 (Table 4, Fig. 4f). These ages are similar to the upper Middle Eocene age determined by the fossil association in the sample (*Subbotina corpulenta*, *S.* aff *jacksonensis*, *Globigerinatheka* spp, *Chiloguembelina* sp, *Turborotalia* sp, *Dentoglobigerina* sp). These are the oldest results reflecting late Eocene-early/late Oligocene volcanism in Grenada, and there are no corresponding K-Ar data. The most abundant zircon populations recovered from beach and river sands in Grenada correspond to this age interval (~ 33 Ma; n: 26), whereas only one grain of this age was recovered on Carriacou.

4.2.5. Zircon older than 40 Ma and xenocrysts

Zircon xenocrysts (in magmatic rocks) and exotic detrital zircon (in sand samples) are most abundant in samples GR23 and GR30 from Grenada, and samples GR42, GR45, SAND 9 and SAND 10 from Carriacou (Tables S3, 1, 4; Fig. 5), but occasional old grains also occur in other samples. The measured dates range from 45.7 ± 1.6 (SAND 9) to 3469 ± 41 Ma (GR30) and are now described from young to old.

In terms of their morphology and CL images (e.g. Fig. 9d), much of the zircon aged 40–160 Ma is indistinguishable from the magmatic zircon derived from crystallization during volcanic events in the southernmost Lesser Antilles. Zircon from sands is more difficult to

interpret because the morphologies and CL images of detrital grains are generally more variable than in samples of volcanic origin, and rounding through mechanical transport can obscure the original morphology. The youngest grains are just slightly older than zircon reflecting the 33–34 Ma volcanic event and only occur in Carriacou in sample SAND9 (41.8–61.4 Ma, Fig. 2; Table S3). These may reflect early Paleocene-middle Eocene volcanism whose volcanic products are concealed by the younger flows, and the zircon may have been picked up during ascent of the younger lavas or, alternatively, it might have been transported in pumice by currents. Volcanic rocks with a K-Ar age of ~45 Ma, for example, are exposed on the Los Testigos islets west of Grenada (Santamaria and Schubert, 1974). Moreover, middle Eocene pillow basalt (Mayreau Basalt, Anse Bandeau Formation, Cherry Hill Basalt) occurs north of the island (Speed et al., 1993).

One Late Jurassic detrital grain was found in sample SAND9 (159.1 ± 3.7 Ma). Its origin is difficult to establish because of a lack of comparable ages in this part of the Lesser Antilles. However, Late Jurassic volcanic rocks on La Désirade, ~200 km north of Grenada (Mattinson et al., 2008), point to the (partial) existence of Mesozoic proto-arc basement in (some of) the Lesser Antilles. Xie and Mann (2014) measured detrital zircon ages in Cenozoic clastic sedimentary rocks of Trinidad, 250 km south of Grenada, and also found relatively rare Jurassic grains with LA-ICP-MS $^{206}Pb/^{238}U$ ages of 150-194 Ma (see their Tables 3 and 4, samples S4 and S5). Goldstein et al. (1997) reported 49 SHRIMP-derived detrital zircon ages for a sand sample collected in the lower Orinoco River in Venezuela and also found rare Jurassic grains that presumably come from the Andes.

Volcaniclastic sample GR45 from Carriacou contains 2 zircon grains with dates of ~220 Ma (Fig. 4d), and a xenocrystic grain dated at 246 ± 8.5 Ma was recovered from dacite sample GR23 from central Grenada (Fig. 4e). This Triassic zircon is also difficult to interpret because rocks of this age are not known from the region. Xie and Mann (2014) found rare Triassic zircon in their survey of Trinidad sediments, but grains of such age were not found in the Orinoco sand investigated by Goldstein et al. (1997). One late Carboniferous zircon found in SAND9 from Carriacou (315.9 ± 8.2 Ma) may also be derived from sources similar to those suggested by Xie and Mann (2014) for rare zircon of similar age from Cenozoic clastic sediments in Trinidad. A few Carboniferous detrital zircon grains were also reported by Goldstein et al. (1997) from an Orinoco sand sample.

Late Ordovician to early Silurian zircon dates are more common in our Grenada samples, occurring in samples GR23 (427–458 Ma, Fig. 5a) and GR15 (410 ± 14 Ma). Detrital zircon grains with such ages also occur in Cenozoic sediments of Trinidad (Xie and Mann, 2014) but

were not reported from the Orinoco River. Only 3 Neoproterozoic zircon grains were found in our xenocrystic and detrital populations—those are from Grenada andesite sample GR23 (778 ±2 6 Ma; Fig. 5a) and Carriacou SAND10 (561 ± 8 and 659 ± 11 Ma). Such grains are more abundant in the Trinidad sediments (Xie and Mann, 2014), and rare early Neoproterozoic zircon also occurs in the Orinoco sand sample of Goldstein et al. (1997).

Considerably older zircon is more abundant in our samples, in line with the findings of Xie and Mann (2014) for Trinidad sediments and the Orinoco sands of Goldstein et al. (1997). A first group seems to characterize a Grenville-age or slightly older source and is represented by grains in the following samples from Carriacou: 4 grains from GR42 (1155 ± 41, 1358 ± 48, 1387 ± 52, 1400 ± 49 Ma; Fig. 5d), one grain in SAND9 (1032 ± 21 Ma) and 3 grains in SAND10 (1131 ± 30, 1221 ± 34, 1353 ± 35 Ma). Similar ages, clustering at 0.9–1.4 Ga, were reported by Xie et al. (2010) from Trinidad sediments and the Orinoco sand sample of Goldstein et al. (1997). These grains are possibly derived from an Andean source (Xie and Mann, 2014).

Two grains are slightly older and represent a late Mesoproterozoic early Paleoproterozoic period in which magmatic events are rare in the region. One xenocryst was found in andesite sample GR23 (1634 ± 8 Ma), and the other is a detrital grain in SAND10 from Carriacou (1544 ± 50 Ma). Such ages were also discovered in the Trinidad sediments (Xie et al., 2010; Xie and Mann, 2014) and in the Orinoco sand. Xie and Mann (2014) speculated that they may reflect magmatism in the northern part of the Guyana Shield. Indeed, there are abundant Mesoproterozoic rapakivi-type granites in both the Guyana and Amazon cratons (for details see Dall'Agnol et al., 1999), and these could have been the source for zircon of the same age on Grenada.

A few late Paleoproterozoic detrital dates almost certainly reflect derivation of zircon from the Guyana Shield (Théveniaut et al., 2006 and references therein; Vanderhaeghe et al., 1998). These rare detrital grains occur in samples SAND9 (2036 ± 44 Ma) and SAND10 (1964 ± 23, 2065 ± 22 Ma). Such dates are more abundant in the Trinidad sediments and also in the Orinoco sand sample of Goldstein et al. (1997). We found only one xenocrystic zircon of middle Paleoproterozoic age in andesite sample GR23 (2218 ± 8 Ma). Such ages are very rare in the Orinoco sand and in the Trinidad sediments referred to above. Derivation from the Guyana Shield is most likely. Finally, we found several Archaean xenocrystic and detrital zircon grains, and some of these are much older than in the Orinoco sand and in the Trinidad sediments. Sample GR42 from Carriacou contains a late Archaean xenocryst (2692 ± 38 Ma), whereas sample SAND10 contained two detrital grains at 2682 ± 18 and 2731 ± 28 Ma. Late

Archaean zircon ~ 2.8 Ga in age was also found in the Orinoco sand (Goldstein et al., 1997), and 3 grains were reported from the Trinidad sediments (Xie and Mann, 2014), most likely derived from the Guyana Shield. The two oldest detrital grains were found in sample GR30, a pyroclastic tuff from central Grenada (Fig. 2). It yielded concordant or near-concordant $^{207}Pb/^{206}Pb$ dates of 3442 ± 42 and 3469 ± 41 Ma respectively (Fig. 5c). The oldest zircon found in the Trinidad sediments was 3253 ± 16 Ma (Xie and Mann, 2014). Nadeau et al. (2013) reported several Paleoarchaean as well as one Hadean zircon xenocryst from Paleoproterozoic felsic volcanic rocks of the Kanuku Complex in the southern Guyana Shield and postulated the existence of a Hadean- to Archean crustal domain at depth. It is possible that our two oldest zircon grains also reflect this ancient basement.

4.3. Zircon Lu-Hf isotopes

Lu-Hf isotopic analysis of dated zircon can help to constrain the relative contributions of juvenile crust (derived from the mantle) and continental crust in the crystallization of this mineral (e.g., Belousova et al., 2006). Initial $^{176}Hf/^{177}Hf$ ratios significantly above those predicted by the chondritic mantle evolution model (i.e. positive $\varepsilon_{Hf(t)}$-values) generally indicate a juvenile input from the depleted mantle, such as is generated during subduction-induced island arc magmatism, or melting of relatively young mantle-derived mafic (underplated?) lower crust.

Negative $\varepsilon_{Hf(t)}$ values generally provide evidence for magma and zircon derived through melting of old (or recycled) continental crust, whereas intermediate values around zero may be indicative of magma and zircon formation from mixing of old crust and depleted mantle-derived material. Significant variations in the Hf isotopic composition of zircon from the same igneous rock usually indicate a heterogeneous source and/or magma mixing in the production of a pluton (Belousova et al., 2006; Kröner et al., 2014; Tang et al., 2014).

The samples selected for Hf isotopic analysis were representative of the very young zircon generations (GR5, 240 ± 12; GR12, 1020 ± 28 ka), as well as of the ~ 5 Ma generation (GR1) and the ~ 32 Ma age group (GR6). Each of these can be related directly to zircon crystallization during Grenada arc volcanism. In addition, Hf isotopes were analyzed in xenocrystic zircon from andesite sample GR23. All these analyses (Table S8, Fig. 10) were performed by LA-ICP-MS in Hong Kong. The analytical procedures are described in the Supplementary Material B.

All zircon directly related to arc magmatism has similar isotopic features, i.e., its $\varepsilon_{Hf(t)}$ values are positive and thus seem to reflect derivation from a predominantly juvenile depleted mantle source, as would be expected in an intra-oceanic arc, and from the majority of the whole-rock Sm-Nd isotopic data (Dhuime et al., 2011). Individual $\varepsilon_{Hf(t)}$ values vary considerably however, indicating significant Hf isotopic heterogeneity in the juvenile zircon source. Zircon grains from sample GR5 exhibits relatively little variation in $\varepsilon_{Hf(t)}$ values, between just under 5 and 7.5 (Table S8, Fig. 10a), zircon from sample GR1 is more heterogeneous ($\varepsilon_{Hf(t)}$ between 2.5 and 8: Table S8, Fig. 10a), and zircon from the ~32 Ma generation in sample GR6 is the most heterogeneous of all ($\varepsilon_{Hf(t)}$ between 4.2 and 13.9: Table 10, Fig. 10b). A similar range in whole-rock Sm-Nd $\varepsilon_{Nd(t)}$ values has been reported by Dhuime et al. (2011) for the Lesser Antilles arc.

In contrast, the xenocrystic zircon grains, have a wide range of $\varepsilon_{Hf(t)}$ values between -16 for a ~ 200 Ma grain and 0 for a ~ 1.4 Ga grain (Table S8, Fig. 10c). These grains predominantly reflects a crustal history, although two of the old zircon from our study may also suggest involvement of a juvenile source (Fig. 10c).

4.4.Zircon trace element composition

The trace element composition of zircon is helpful for the reconstruction of magmatic histories and fingerprinting of magma sources (Grimes et al., 2007; Burnham and Berry, 2012). For this study this has proved to be a useful tool in differentiating between different types of magma generated by Grenada volcanism through time. The trace element data were collected by LA-ICP-MS (Mainz laboratory) from the same (or adjacent) CL-domains used for SHRIMP analysis. For the sand samples (SAND1 to 14), U-Pb dating and trace element analyses were conducted simultaneously by LA-ICP-MS (Beijing laboratory; Table S9). Chondrite-normalized REE values are plotted by age range in Fig. 11.

4.4.1. <2.0 Ma and 5–20 Ma (Recent arc)

The younger Lesser Antilles arc has been active since the early Burdigalian (22–19 Ma) (Bouysse et al., 1990 and references therein). Zircon in the < 2.0 Ma age range is the most abundant in Grenada, less so in Carriacou, and absent, most probably due to sampling bias, on Petite Martinique. More than 250 trace element analyses were obtained for zircon of this age group, and 40 for the 5–20 Ma age group (Figs. 11a, b). Both age groups mostly display similar REE patterns. The analyses show slight negative Eu anomalies (Eu/Eu* = 0.66–0.63;

Table S9), well-defined positive Ce anomalies, and a marked enrichment in HREE. These compositions are consistent with crystallization from very oxidized (~ 2 to 3 $\log_{10}$ orders fO_2 > synthetic nickel-nickel oxygen buffer) magmas in which Eu^{2+} was extremely limited in abundance (Trail et al., 2012; Burnham and Berry, 2012).

4.4.2. ~27–56 Ma (Older arc)

The older arc was active from the beginning of the early Eocene to the mid-Oligocene (30–28 Ma) (Bouysse et al., 1990 and references therein). The REE signatures from zircon within this age range are markedly different from those of the younger arc and display two different patterns (Figs. 11c, d). The first pattern exhibits enriched HREE, moderately developed positive Ce anomalies and negative Eu anomalies (Eu/Eu* = 0.27; Table S9). The second pattern shows enrichment in a portion of the LREE, smaller to no Ce anomalies, and negative Eu anomalies (Eu/Eu* = 0.20; Table S9). Two older grains (~ 61 and 68 Ma) show the same signature as the second pattern. The combination of positive Ce and negative Eu anomalies in this zircon population indicates crystallization from magmas that were variably but considerably less oxidized than those of the younger southern arc.

4.4.3. >150 Ma (up to ~2600 Ma)

This group corresponds to xenocrystic grains not related to the arc of the Lesser Antilles. However, the REE signature is similar to the first pattern of the ~27–68 Ma group (Fig. 10c) with moderately developed positive Ce anomalies, negative Eu anomalies (Eu/Eu* = 0.27), and enrichment in HREE (Fig. 11e; Table S9).

5. Discussion

5.1.Paleogeographic constraints

The Orinoco River drains the northern South American continent and is the main source of terrigenous sediment in the Lesser Antilles (Westbrook et al., 1984; Aslan et al., 2003). Sediments are derived from different source regions within its watershed, including the Andes to the west, the northern Venezuela coastal ranges, and the Guyana Shield. The geologic history of the Orinoco River is intrinsically related to the evolution of the southern Lesser Antilles since clastic sedimentary material entered the forearc basin from the south and the Antilles trench/Barbados accretionary prism from the east. Therefore in order to locate the provenance of the old/xenocristic zircon found in Grenada and Carricou the evolution of this river system must be assessed.

Previous studies suggested that a large north-northwest paleofluvial system drained through the present Maracaibo Basin (Venezuela) during pre-Oligocene times (Kasper and Larue, 1986; Hoorn et al., 1995; Escalona and Mann, 2006; Xie et al., 2010; Noguera et al., 2011). Uplift of the Colombian Andes and the Merida Andes of Venezuela (western and central Cordillera, Fig. 12, including the northern Venezuela coastal ranges) deflected the paleofluvial system eastwards. The changing paleogeography from the early Eocene (~50 Ma) to Pliocene (~5 Ma), based on the work of Escalona and Mann (2011; see also Pindell et al., 2005), can be used to reconstruct the evolution of the river system. Simplified versions of such maps, showing only key geologic features related to the magmatic evolution of the Cenozoic Antilles arc and the likely provenance of the old zircon grains are illustrated in Fig. 12 and discussed in section 5.4.

5.2. Age of arc magmatism in the southern lesser Antilles

The single zircon U-Pb ages in the present study corroborate and define the age of arc-volcanism in the southern Lesser Antilles (Grenada, Carriacou and Petite Martinique) and define an upper (late Eocene; ~34 Ma) and lower age limit (late Pleistocene; 241 ± 12 ka). Note that active (submarine) volcanism persists offshore of the north Grenada coast at Kick'em Jenny (Fig. 1b; Devine & Sigurdsson, 1995). Evidence for the oldest volcanic activity comes from zircon grains (~34–29 Ma) found in samples from the Tufton Hall (Grenada) and the Belvedere (Carriacou) Formations. Even though the sites of Eocene island arc rocks are unknown, the presence of zircon with almost the same age as the depositional age of the two units and of fresh pyroxene grains (Saunders et al., 1985) suggest igneous activity very close to the sedimentary basin (Fig. 12a). Paleogene magmatic rocks have been described north of Grenada (middle Eocene pillow basalt) and in Carriacou (upper Oligocene basalt of the Belvedere Formation), but such occurrences may not be a product of Paleogene arc magmatism, but of a spreading event related to the formation of oceanic lithosphere in the southern Grenada Basin (Speed et al., 1993). It is important to note that the REE signatures from zircon within this age range are markedly different from those of the younger (Neogene to late Pleistocene) zircon suggesting a different magmatic history.

The occurrence of Neogene zircon grains in our samples point to local middle Miocene active subaerial volcanoes with volcanic centers located in and near Petite Martinique. From the Late Miocene to Late Pleistocene volcanic centers were particularly active, with the generation of copious magmatism.

5.3. Zircon xenocryst provenance in volcanic rocks of the southern Lesser Antilles

The extent of subducted sediment input into the mantle wedge in the Lesser Antilles remains controversial (Devine, 1995; Thirlwall et al., 1996; Carpentier et al., 2008, Bézard et al., 2014, 2015); some authors argued that the sediment signature of lavas was acquired within the crustal portion of the overriding Caribbean plate during magma ascent rather than from a contaminated source in the mantle wedge (Thirlwall et al., 1996, Van Soest et al., 2002). Chauvel et al. (2012) suggested, however, that beneath the southern part of the Lesser Antilles arc, large volumes of subducted sediment were melted to produce island arc magmas with trace element characteristics and isotopic signatures typical of continental crust, namely low initial $^{143}Nd/^{144}Nd$ and $^{176}Hf/^{177}Hf$ and high initial $^{87}Sr/^{86}Sr$ and Pb isotopic ratios. O'Neill (2016) also presented evidence that the elevated LREE/HREE of the Grenada magmas derives from sediment contamination of wedge sources rather than residual garnet in the source.

In a broad sense, the zircon xenocrysts identified in the Grenada and Carriacou volcanic rocks have a similar age distribution to that of detrital zircon recovered from beach and river sands from these islands. This detrital zircon is probably derived from a local source, although input from a more distal source through longshore drift, currents and wave action, at least for the beach samples, cannot be excluded. The xenocrystic zircon with dates around 42–61 Ma found in Carriacou, likely represent early Paleocene to Eocene volcanic rocks in the subsurface of the southern Lesser Antilles.

On the other hand, the ages and geochemical composition of the older xenocristic grains in our samples are broadly consistent with ultimate derivation from northern South America. The histograms in Figure SM16 compare our xenocristiczircon results with zircon dates from nearby regions such as the Barbados, Trinidad, the Orinoco River and the Maracaibo basin. The purpose of showing the histogram is to present the ages from nearby regions rather than exact correlations with the ages we obtained. In our opinion the lack of peak concordance is more the result of statistically limited sampling than a real correlation. Whether the xenocristiczircon was introduced into the rocks of the southern Lesser Antilles arc by incorporation of subducted sediments into the mantle source rocks or through crustal assimilation is the salient question.

5.3.1. Incorporation of inherited zircon into the mantle source via subducted sediment

One possibility for the incorporation of older zircon into the arc-magmas is that the grains were originally deposited on the subducting Atlantic ocean crust (North American plate), possibly transiting via the Barbados accretionary prism. Evidence of arc contamination by

subducted terrigenous sediments is well-documented in the Lesser Antilles island arc (e.g. Carpentier et al., 2008, 2009). According to Carpentier et al., (2009) zircon-rich clastic (coarse) sediments deposited next to the South American continent have very low whole-rock $\varepsilon_{Hf(t)}$ values inherited from old zircon. These sediments, which were also subducted below the intra-oceanic arc, have "continental" isotopic ratios and their presence has been used as a strong argument for the extreme isotopic compositions of the arc lavas (Carpentier et al., 2008; 2009).

Taking into account the strong petrogenetic evidence from the present study that the magmas hosting xenocrystic zircon are derived predominantly through fractional crystallization of primitive (high liquidus temperatures) basaltic parents, a subducted zircon source seems unlikely. Furthermore, the absence of negative Eu anomalies in the Grenada suite is inconsistent with any involvement of partially melted, detrital Proterozoic and younger subducted sediment. The latter, although characterized by high La/Yb_N, would also have strong negative Eu anomalies. Arculus (1978) documented the occurrence of quartz grains with reaction coronae of clinopyroxene in many of the M and C series basalts of Grenada. Quartz grains are better interpreted as partially assimilated intra-crustal material rather than recycled detritus from a subducted sedimentary source. We therefore support the conclusions of Bezard et al. (2014) who have suggested that subducted sedimentary material has not been a major factor in causing major isotopic heterogeneity in the Lesser Antilles arc lavas.

5.3.2. Incorporation of zircon by assimilation of crustal material

Bezard et al. (2014) favored crustal sediment assimilation (up to 20–40%) in the Lesser Antilles volcanic rocks related to storage of magma in (and/or passage through) the associated pre-Oligocene sedimentary basin. Intra-arc basins are present in Martinique and St Lucia, and sediments of the Tufton Hall Formation of Grenada and the Belvedere Formation of Carriacou are potentially one of the local intra-arc zircon-bearing sources through which the younger arc magmas were emplaced. Even though the nature of the basement of the Southern Lesser Antilles arc is poorly known, Aitken et al. (2011) suggested that the central-southern Lesser Antilles arc developed above a deep fore-arc basin of the (now extinct) Aves Ridge Arc. The sediments that filled the $\leq$ 13 km-thick fore-arc basin originated from the nearby South American continent and were transported fluvially from regions as far away as the northern Andes of Colombia and Venezuela. Xenocrystic zircon morphology argues for a sedimentary origin (e.g., Fig. 8d).

Bezard et al. (2014) proposed a schematic model for the Soufrière Volcanic Complex (St Lucia) showing active assimilation of sediments at shallow depths. A similar scenario was envisaged for Grenada in which Thirlwall et al. (1996) suggested from a Pb isotope study that the composition of Grenada magmas is strongly affected by high-level crustal assimilation. Most probably some of the old zircon dissolved, and the melt became saturated in zirconium and crystallized new zircon grains. Preservation of old crystals is favored in cases of relatively short residence time in crustal chambers (Bea and Montero, 2013).

5.4. Evolution of the Lesser Antilles region: A zircon perspective

During the *early Eocene (~ 50 Ma)*, deep-water sedimentation began in the proto-Barbados accretionary prism and Tobago-Grenada forearc basin in the Proto-Caribbean (Escalona and Mann, 2011). The fluvial-deltaic complex of the proto-Maracaibo River was in close proximity to the proto-Barbados accretionary wedge (Fig. 12a). This proximity suggests that the xenocristiczircon in Grenada and Carriacou (up to Grenville age) was probably derived from the central Andean Cordillera. Even though most clastic material was entering the forearc basin from the south (Aitken et al., 2011), uplifted Caribbean terranes (Great arc of the Caribbean) were also localized sources of clastic sediments (Xie at al., 2010; Escalona and Mann, 2011). Such arc-derived volcanogenic sediment began to accumulate on the oceanic crust and its pelagic cover between ~ 43 and 46 Ma (middle Eocene; Speed et al., 1993). This sedimentation and the basin environment persisted through the Oligocene.

During the Oligocene *(~30 Ma)*, the Caribbean plate moved eastwards relative to South America, triggering a series of tectonic events that completely modified the paleodrainage systems and basin fill along the entire northern South American margin (Escalona and Mann, 2011). Isostatic rebound of the Maracaibo basin and uplift of Caribbean terranes created geomorphologic barriers that diverted north-directed paleodrainages towards the east into the present-day area of the Orinoco delta (Fig. 12b). To the east, the proto Grenada-Tobago forearc basin was split into two basins by the rising Lesser Antilles arc. The main Oligocene source rocks include: 1) deep water terrigenous shales derived from the continent and deposited in the eastern Venezuela and Trinidad basins; and 2), terrigenous shales derived from the assembled Caribbean terranes and deposited into the forearc basin depocenters. At this stage, sediments continued to originate primarily from the south, as demonstrated by our sample from the Belvedere Formation in Carriacou (GR45) in which old zircon with ages between 200 and 500 Ma suggests derivation from the western Andes of Venezuela and Colombia.

Even though there are many volcanic-derived sediments from this period, there was no magmatism of demonstrable arc origin within the fore-arc sedimentary basin until initiation of volcanism of the Neogene arc, which was underway at about 14 Ma (Speed et al., 1993). Only minor volumes of basalt of uncertain tectonic affinity extruded within the sediments of the Belvedere Formation (Speed et al, 1993).

Oblique convergence in Miocene times (14 Ma) between the Caribbean and South American plates in the Trinidad area induced final uplift of the rising Lesser Antilles arc and final separation of the Grenada and Tobago basins in the southeastern Caribbean (Aitken et al., 2011). The proto-Orinoco system collected the east-directed drainages of the eastern Cordillera, the south-directed drainages of the Merida Andes and Cordillera de la Costa, and the north-directed drainages of the Guyana shield to become the largest paleodrainage system in northern South America (Fig. 12c). On the other hand, from the early Miocene, a large part of the drainage of northwest Amazonia was directed northward along the paleo–Orinoco river system to a delta in Lake Maracaibo. Uplift of the Eastern Cordillera in the late middle Miocene initiated development of the Amazon River. No connection with the Atlantic was established, however, and the Amazon fed the paleo–Orinoco river system, which drained toward the Caribbean (Hoorn et al., 1995). To the northeast of the basin, alluvial fan deltas, deep-water turbidites and mass transport complexes were deposited into the foreland basin (Rodriguez, 1999). The Mesoproterozoic and Archean xenocristiczircons found in porphyritic tuff sample GR30 from Grenada and the volcanic-derived sample GR42 from the Grand Bay Formation in Carriacou suggest derivation from the Guyana shield. Samples GR30 and GR42 are coarse- to medium-grained, respectively, and indicate a dynamic geological setting in close proximity to the sedimentary basin. The detrital zircon analysis reveals a likely nearby source. The old zircon grains most likely come from a volcanic rock that picked up the ancient grains during magma ascent and was later eroded. The erosional products were deposited in the basin. The Lesser Antilles arc continued to develop during the late Miocene-early Pliocene to the present. This phase is similar to the present-day geography of the South America-Caribbean margin, with the continued development of a major right-lateral transform fault (El Pilar) between the Caribbean and the South American plates (Fig. 12d).

During the late Miocene (Aitken 2011), the Grenada and Tobago basins were divided by the emergent Lesser Antilles arc and associated inverted forearc crust between Margarita Island and Grenada. The Tobago basin received significantly more sediment influx from the proto-Orinoco River, which almost filled the southern parts of the basin to sea level. The Grenada basin developed a strongly symmetrical depocenter, with sediments coming

primarily from the Neogene Lesser Antilles arc as demonstrated by our 41–60 Ma grains in sand samples derived from the Great Arc of the Caribbean.

6. Conclusions

The single zircon U-Pb ages in the present study corroborate and define the age of arc-volcanism in the southern Lesser Antilles (Grenada, Carriacou and Petite Martinique) and define an upper (late Eocene; ~34 Ma) and lower age limit (late Pleistocene; 241 ± 12 ka), although active volcanism continues off-shore of Grenada. Since most zircon grains in our study are younger than 2 Ma, a new analytical procedure was developed to correct for lack of secular equilibrium in the ^{238}U decay chain.

The trace element characteristics of the zircon clearly differentiate between different types of magma generated during southern Lesser Antilles volcanism through time between the younger arc (Miocene, ~22–19 Ma) and older arc (Eocene to mid-Oligocene, ~30–28 Ma). All igneous zircon has positive $\varepsilon Hf(t)$, reflecting derivation from a predominantly juvenile mantle source. However, the $\varepsilon Hf(t)$ values vary considerably within samples, reflecting considerable Hf isotopic heterogeneity in the source rocks.

Our study of zircon from the islands of Grenada, Carriacou and Petite Martinique shows, for the first time, the presence of Paleozoic and Paleoarchean (250–3469 Ma) xenocrysts within late Paleogene to Neogene (~34–0.2 Ma) volcanic rocks and late Jurassic to Precambrian zircons (158–2667 Ma) in beach and river sands. These findings together with the geochemistry of the rocks containing zircons provide strong evidence for the assimilation of detrital sediments from the intra-arc proto-Grenada/Tobago basin. Paleogeographic reconstructions show that the old detrital zircons could have been derived from distant regions such as the Eastern Andean Cordillera of Colombia, the Merida Andes, and the northern Venezuela coastal ranges, transported first by the Proto-Maracaibo and proto-Orinoco rivers.

Acknowledgments

YRA thanks Bob Stern for suggesting fieldwork in Grenada to “hunt” for old zircons”. Liqin Zhou and Xiao-Chao Che provided the zircon CL images, Chun Yang prepared perfect zircon mounts, and Jianhui Liu and Zhiqing Yang made sure that the SHRIMP II instrument in Beijing was in excellent operating conditions. Jianfeng Gao of Nanjing University provided an unpublished Excel-based program to construct the Hf evolution diagrams of Fig. 9. This study was supported by Deutsche Forschungsgemeinschaft (DFG) grants KR590/85-1 to AK and RO4174/2-1 to YRA, and Spanish MINECO grants CGL2015-65824 and CGL2012-

36263 and University of Granada research program (CIC) to AGC and CLC. This research also received support from the SYNTHESYS Project (http://www.synthesys.info/) which is funded by the European Community Research Infrastructure Action under the FP7 "Capacities" Program, the Intra-University Research Support Program of Mainz University (Universitätsinterne Forschungsförderung (FoFö). We thank two anonymous reviewers who helped to improve the manuscript and Prof. Sun (editor of LITHOS) for handling our publication.

References

Aguillón-Robles, A., Calmus, T., Benoit, M., Bellon, H., Maury, R.O., Cotten, J., Bourgois, J., Michaud, F., 2001. Late Miocene adakites and Nb-enriched basalts from Vizcaino Peninsula, Mexico: indicators of East Pacific Rise subduction below Southern Baja California? Geology 29, 531–534.

Aitken, T., Mann, P., Escalona, A., Christeson, G.L., 2011. Evolution of the Grenada and Tobago Basins and implications for arc migration. Mar. Pet. Geol. 28, 235–258.

Arculus, R. J., 1973. The alkali basalt, andesite association of Grenada, Lesser Antilles. Unpublished Ph.D. thesis, Durham University, UK

Arculus, R.J., 1976. Geology and geochemistry of the alkali basalt—andesite association of Grenada, Lesser Antilles island arc. Geological Society of America Bulletin 87, 612-624.

Arculus, R.J., 1978. Mineralogy and petrology of Grenada, Lesser Antilles island arc. Contributions to Mineralogy and Petrology 65 413-424.

Arculus R. J. 1994. Aspects of magma genesis in arcs. Lithos 33, 189–208

Arculus, R.J., 2004. Evolution of arc magmas and their volatiles. In: Sparks, R.S.J., Hawkesworth C.J. (eds.). The state of the planet: frontiers and challenges in geophysics. Washington DC: American Geophysical Union, 150, 95-108.

Aslan, A., White W., Warne A., Guevara E.H., 2003. Holocene evolution of the Western Orinoco delta, Venezuela. Geological Society of America Bulletin 115, 479-498.

Bateman, H., 1910. Solution of a system of differential equations occurring in the theory of radioactive transformations. Proc Cambridge Phil Soc 15:423-427.

Bea, F., Montero, P., 2013. Diffusion-induced disturbances of the U–Pb isotope system in pre-magmatic zircon and their influence on SIMS dating. A numerical study. Chemical Geology 349-350, 1-17.

Beard, J. S., Ragland, P. C., Crawford, M. L.,2005. Reactive bulk assimilation: A model for crust–mantle mixing in silicicmagmas. Geology 3, 681–684.

Behn, M.D., Kelemen, P.B., Hirth, G., Hacker, B.R., Massonne, H.J., 2011. Diapirs as the source of the sediment signature in arc lavas. Nature Geoscience 4, 641–646.

Belousova, E.A., Griffin, W.L., O'Reilly, S.Y., 2006. Zircon crystal morphology, trace element signatures and Hf isotope composition as a tool for petrogenetic modelling: examples from eastern Australian granitoids. Journal of Petrology 47, 329–353.

Bezard, R., Davidson, J. P., Turner, S., Macpherson, C. G., Lindsay, J. M., Boyce, A. J., 2014. Assimilation of sediments embedded in the oceanic arc crust: myth or reality? Earth and Planetary Science Letters 395, 51–60.

Bezard, R., Turner, S., Davidson, J.P., Macpherson, C.G., Lindsay, J.M. 2015. Seeing through the effects of crustal assimilation to assess the source composition beneath the southern Lesser Antilles Arc. Journal of Petrology 56, 815-844.

Bird, P., 2003. An updated digital model of plate boundaries, Geochem. Geophys. Geosyst., 4(3), 1027. doi:10.1029/2001GC000252.

Black, L.P., Jagodzinski, E.A., 2003. Importance of establishing sources of uncertainty for the derivation of reliable SHRIMP ages. Australian Journal of Earth Sciences 50, 503–512.

Bouysse, P., 1984. The Lesser Antilles island arc: structure and geodynamic evolution. In Biju-Duval, B., Moore, J. C. et al. (eds.) Initial Reports. DSDP 78A. Washington, U.S. Governmentt. Printing Office, 83-103.

Bouysse, P., Westercamp, D., and Andreieff, P., 1990. The Lesser Antilles island arc. In Moore, J.C., Mascle, A., et al., Proc. ODP, Sci. Results, 110: College Station, TX (Ocean Drilling Program), 29–44. doi:10.2973/odp.proc.sr.110.166.1990

Bouysse, P., Westercamp, D., 1990. Subduction of Atlantic aseismic ridges and Late Cenozoic evolution of the Lesser Antilles island-arc. Tectonophysics 175, 349–390.

Bouysse, P., Andreieff, P., Baubron, J.C., Mascle, A., Maury, R.C., Westercamp, D., 1985. Aves Swell and northern Lesser Antilles ridge: rock-dredging results from ARCANTE 3 cruise. Geodynamics of the Caribbean, Symposium. TECHNIP, Paris, 65-76.

Briden, J.C., Rex, D.C., Faller, A.M., Tomblin, J.F., 1979. K–Ar geochronology and pale-omagnetism of volcanic rocks in the Lesser Antilles island arc. Philosophical Transactions of the Royal Society, Mathematics, Physics, Engineering Sciences 291, 485–528.

Burnham, A.D., Berry, A.J., 2012. An experimental study of trace element partitioning between zircon and melt as a function of oxygen fugacity. Geochimica et Cosmochimica Acta 95, 196-212

Caldwell, G. 1983. A study of the volcanic rocks of the southern half of Carriacou, Grenadines, West Indies. Unpublished M.Sc. thesis, University of Windsor, Canada, 158 p.

Caldwell, G., Smith, T.E., Uang, C.H., Jackson, T.A. 1984. The geochemistry and petrogenesis of the volcanic rocks of Carriacou, Grenadine Islands, West Indies. Bulletin Volcanologique 47, 467–482.

Carpentier, M., Chauvel, C., Mattielli, N., 2008. Pb–Nd isotopic constraints on sedimentary input into the Lesser Antilles arc system. Earth and Planetary Science Letters 272, 199–211.

Carpentier, M., Chauvel, C., Maury, R.C., Mattielli, N., 2009. The 'zircon effect' as recorded by the chemical and Hf isotopic composition of Lesser Antilles forearc sediments. Earth and Planetary Science Letters 287, 86–99.

Castro, A., Gerya, T.V., 2008. Magmatic implications of mantle wedge plumes: Experimental study, Lithos 103, 138–148.

Castro, A., Gerya, T.V., García-Casco, A., Fernández, C., Diaz-Alvarado, J., Moreno-Ventas, I., Löw, I., 2010. Melting relations of MORB-sediment mélanges in underplated mantle wedge plumes. Implications for the origin ofcordilleran-type batholiths, Journal of Petrology 51, 1267–1295.

Chauvel, C., Labanieh, S., Carpentier, M., 2012. What does the Lesser Antilles arc tell us about the fate of subducted slabs? Abstract-vol., EGU General Assembly 2012, Vienna, Austria, p. 7108.

Condie, K.C., 2005, TTGs and adakites: Are they both slab melts? Lithos, 80, 33–44.

Dall'Agnol, R., Costi, H.T., Leite, A.A., Magalhães, M.S., Teixeira, N.P., 1999. Rapakivi granites from Brazil and adjacent areas. Precambrian Research 95, 9–39

Defant, M.J., Jackson, T.E., Drummond, M.S., Deboer, J.Z., Bellon, H., Feigenson, M.D., Maury, R.C., Stewart, R.H., 1992. The geochemistry of young volcanism throughout western Panama and southeastern Costa-Rica — an overview. Journal of the Geological Society, London 149, 569–579.

Devine, J.D., 1987. Role of volatiles in Lesser Antilles island arc magmas. Unpublished PhD thesis. University of Rhode Island, USA, 612 p.

Devine, J.D., 1995. Petrogenesis of the basalt-andesite-dacite association of Grenada, Lesser Antilles island arc, revisited: Journal of Volcanology and Geothermal Research. 69, 1–33.

Devine, J.D., Sigurdsson, H., 1995. Petrology and eruption styles of Kick 'em Jenny submarine volcano, Lesser Antilles island arc. J Volcanol Geotherm Res 69:35–58.

Dhuime, B., Hawkesworth, C.J., Cawood, P., 2011. When continents formed. Science 331, 154-155.

De Mets, C., Gordon, R.G., Argus, D.F., 2010. Geologically current plate motions. Geophysical Journal International 181, 1-80.

Donovan, S.K., Pickerill, R.K., Portell, R.W., Jackson, T.A., Harper, D.A.T., 2003. The Miocene palaeobathymetry and palaeoenvironments of Carriacou, the Grenadines, Lesser Antilles. Lethaia, 36, 255–272.

Donovan, S.K., Jackson, T.A., 2013.The Miocene of Carriacou, the Grenadines, Lesser Antilles. Geology Today 29 (4), 150–158.

Escalona, A., Mann, P., 2006. Sequence-stratigraphic analysis of Eocene clastic foreland basin deposits in central Lake Maracaibo using high-resolution well correlation and 3-D seismic data. American Association of Petroleum Geologists, Bulletin 90, 581–623.

Escalona, A., Mann, P., 2011. Tectonics, basin subsidence mechanisms, and paleogeography of the Caribbean–South American plate boundary zone. Marine and Petroleum Geology 28, 8–39.

Geotermica Italiana S.r.l., 1981. Reconnaissance study of the geothermal resources of the Republic of Grenada – Final Report. 126: Latin American Energy Organization.

Gerya, T., Yuen, D., 2003. Characteristics-based marker-in-cell method with conservative site-differences schemes for modeling geological flows with strongly variable transport properties. Physics of the Earth and Planetary Interiors 140, 293–318.

Germa, A., Quidelleur, X., Labanieh, S., Chauval C., Lahitte, P., 2011. The volcanic evolution of Martinique Island: Insights from K-Ar dating into the Lesser Antilles arc migration since the Oligocene, Journal of Volcanology and Geothermal Research 208, 122–135.

Goldstein, S.L., Arndt, N.T., Stallard, R.F., 1997. The history of a continent from U–Pb ages of zircons from Orinoco River sand and Sm–Nd isotopes in Orinoco basin river sediments. Chemical Geology 139, 271–286.

Grimes, C.B., John, B.E., Kelemen, P.B., Mazdab, F., Wooden, J.L., Cheadle, M.J., Hanghøj, K., Schwartz, J.J., 2007. The trace element chemistry of zircons from oceanic crust: a method for distinguishing detrital zircon provenance. Geology 35, 643–646.

Hart, S.R., Blusztajn, J., Dick, H.J.B., Meyer, P.S., Muehlenbachs, K.,1999. The fingerprint of seawater circulation in a 500-meter section of ocean crust gabbros. Geochimica et Cosmochimica Acta 63, 4059–4080.

Hawkesworth, C.J., O'Nions, R.K., and Arculus, R.J., 1979, $^{143}Nd/^{144}Nd$ and $^{87}Sr/^{86}Sr$ geochemistry of the alkalic rock suite, Grenada, Lesser Antilles: Earth and Planetary Science Letters 45, 237–248.

Hacker, B. R., Kelemen, P. B., Behn, M. D., 2011. Differentiation of the continental crust by relamination. Earth and Planetary Science Letters 307, 501–516.

Hofmann, A.W., 1986. Nb in Hawaiian magmas: constraints on source composition and evolution. Chemical Geology 57, 17–30.

Hofmann, A.W., 1988. Chemical differentiation of the Earth: the relationship between mantle, continental crust, and oceanic crust. Earth and Planetary Science Letters 90, 297–314.

Hofmann, A.W., White, W.M., 1982. Mantle plumes from ancient oceanic crust. Earth and Planetary Science Letters 57, 421–436.

Hofmann A.W., Jochum K.-P., Seufert M., White W.M., 1986. Nb and Pb in oceanic basalts: new constraints on mantle evolution. Earth and Planetary Science Letters 79, 33– 45.

Hoorn, C., Guerrero, J., Sarmiento, G.A., Lorente, M.A., 1995. Andean tectonics as a cause for changing drainage patterns in Miocene northern South America. Geology 23, 237–240.

Jackson, T.A., 1980. The composition and differentiation of the volcanic rocks of Carriacou, Grenadines, West Indies. Bulletin of Volcanology 43, 311-324.

Jackson, T.A., Scott, P.W., Donovan, S.K., Pickerill, R.K., Portell, R.W., Harper, D.A.T., 2008. The volcaniclastic turbidites of the Grand Bay Formation, Carriacou, Grenadines, Lesser Antilles. Caribbean Journal of Science 44, 116-124.

Jahn, B.M., Bernard Griffiths, J., Charlot, R., Cornichet, J., Vidal, F., 1980. Nd and Sr isotopic compositions and REE abundances of cretaceous MORB (Holes 417d and 418a, Legs 51, 52 and 53). Earth and Planetary Science Letters 48, 171–184.

Johnson, M.C., Plank, T., 1999. Dehydration and melting experiments constrain the fate of subducted sediments. Geochemistry, Geophysics, Geosystems 1, doi: 10.1029/ 1999GC000014.

Jolly, W.T., Lidiak, E.G., Dickin, A.P., 2006. Cretaceous to mid-Eocene pelagic sediment budget in Puerto Rico and the Virgin Islands (northeast Antilles Island arc). Geologica Acta 4, 35–62.

Kasper, D.C., Larue, D.K., 1986. Paleogeographic and tectonic implications of quartzose sandstones of Barbados. Tectonics 5, 837-854.

Kay, S.M., Ramos, V.A., Marquez, M., 1993. Evidence in Cerro-Pampa volcanic-rocks for slab-melting prior to ridge-trench collision in southern South-America. Journal of Geology 101, 703–714.

Kelemen, P.B., Hanghøj, K., Green, A.R., 2003. One view of the geochemistry of subduction related magmatic arcs, with an emphasis on primitive andesite and lower crust. In:

Rudnick, R. (ed.), Geochemistry of the crust: Treatise of geochemistry. Elsevier, Amsterdam, pp. 593–659.

King, R.L., Bebout, G.E., Moriguti, T., Nakamura, E., 2006. Elemental mixing systematics and Sr–Nd isotope geochemistry of melange formation: Obstacles to identification of fluid sources to arc volcanics. Earth and Planetary Science Letters 246, 288–304.

Kröner, A., Kovach, V., Belousova, E., Hegner, E., Armstrong, R., Dolgopolova, A., Seltmann, R., Alexeiev, D.V., Hoffmann, J.E., Wong, J., Sun, M., Cai, K.,Wang, T., Tong, Y.,Wilde, S.A.,Degtyarev, K.E.,Rytsk, E., 2014. Reassessment of continental growth during the accretionary history of the Central Asian Orogenic Belt. Gondwana Research 25, 103–125.

Labanieh, S., Chauvel, C., Germa, A., Quidelleur, X., Lewin, E., 2010. Isotopic hyperbolas constrain sources and processes under the Lesser Antilles Arc. Earth and Planetary Science Letters 298, 35–46.

Le Bas, M.J., Le Maitre, R.W., Streckeisen, A., 1986. A chemical classification of volcanic rocks based on the total alkali-silica diagram. Journal of Petrology 27, 745-750.

Macdonald, R., Hawkesworth, C.J., Heath, E., 2000. The Lesser Antilles volcanic chain: a study in arc magmatism. Earth-Science Reviews 49, 1–76.

Mann, U., Schmidt, M.W., 2015. Melting of pelitic sediments at subarc depths: 1. Flux vs. fluid-absent melting and a parameterization of melt productivity. Chemical Geology 404, 150-167.

Marschall, H,R., Schumacher, J.C., 2012. Arc mafmas sourced from mékange diapirs in subduction zones. Nature Geoscience 5, 862-867.

Mattinson, J.M., Pessagno, E.A. Jr, Montgomery, H., Hopson, CA., 2008. Late Jurassic age of oceanic basement at La Désirade Island, Lesser Antilles arc. Geological Society of America, Special Papers 438, 175-190.

McDonough, W.F., Sun, S.-S., 1995. The composition of the Earth, Chem. Geol., 120, 223 – 253.

Münker, C., Wörner, G., Yogodzinski, G., Churikova, T., 2004. Behaviour of high field strength elements in subduction zones: constraints from Kamchatka–Aleutian arc lavas. Earth and Planetary Science Letters 224, 275-293.

Nadeau, S., Chen, W., Reece, J., Lachhman, D., Ault. R., Lins Faraco, M.T., Fraga, L.M., Reis, N.J., Betiollo, L.M., 2013. Guyana: the lost Hadean crust of South America? Brazilian Journal of Geology 43, 601-606.

Nelson, D.R., 1997. Compilation of SHRIMP U–Pb Zircon Geochronology Data, 1996. Geological Survey of Western Australia, Record 1997/2, 189 pp.

Noguera, M.I, Wright, J.E., Urbani, F., Pindell, J., 2011. U-Pb geochronology of detrital zircons from the Venezuelan passive margin: implications for an Early Cretaceous Proto-Orinoco river system and Proto-Caribbean ocean basin paleogeography. Geologica Acta 9, 265-272.

O'Neill, H.St.C., 2016. The Smoothness and Shapes of Chondrite-normalized Rare Earth Element Patterns in Basalts. Journal of Petrology 57, 1463–1508.

Parkinson, I.J., Arculus, R.J., Eggins, S.M., 2003. Peridotite xenoliths from Grenada, Lesser Antilles island arc. Contributions to Mineralogy and Petrology 146, 241-262.

Pearce, J.A., 2008. Geochemical fingerprinting of oceanic basalts with applications to ophiolite classification and the search for Archean oceanic crust. Lithos 100, 14-48.

Pindell, J., Kennan, L., Maresch, W.V., Stanek, K.-P., 2005. Plate-kinematics and crustal dynamics of circum-Caribbean arc-continent interactions: Tectonic controls on basin development in Proto-Caribbean margins. Geological Society of America, Special Papers 394, 7-52.

Plank, T., Langmuir, C.H., 1998. The chemical composition of subducting sediment and its consequences for the crust and mantle. Chemical Geology 145, 325-394.

Richardson, P.L., 2005. Caribbean Current and eddies as observed by surface drifters. Deep Sea Research Part II: Tropical studies in oceanography 52, 429-463.

Robertson, R.E.A., 2005, Grenada. In: Lindsay, J.M., Robertson, R.E.A., Shepherd, J.B., Ali, S., (eds.), Volcanic hazard atlas of the Lesser Antilles: Trinidad and Tobago, Seismic Research Unit, University of the West Indies, p. 50–66

Robinson, E., Jung, P., 1972. Strartigraphy and age of marine rocks, Carriacou, West Indies. American Association of Petroleum Geologists, Bulletin 56, 114-127.

Rodriguez, L., 1999. Tectonic analysis, stratigraphy and depositional history of the Miocene sedimentary section, central eastern Venezuela basin. Unpublished PhD thesis, University of Texas at Austin, Austin, TX, USA, 119 p.

Rojas-Agramonte, Y., Garcia-Casco, A., Kemp, A., Kröner, A., Proenza, J.A., Lázaro, C., Liu, D., 2016. Recycling and transport of continental material through the mantle wedge above subduction zones: A Caribbean example. Earth and Planetary Science Letters 436, 93-107.

Sakata, S., Hirakawa, S., Iwano, H., Danahara, T., Hirata, T., 2013. Correction of initial disequilibrium on U-Th-Pb system for dating young zircons – Goldschmidt Conference

Abstracts 2013. Mineralogical Magazine, 77, 2116.

Samaniego, P., Martin, H., Monzier, M., Robin, C., Fornari, M., Eissen, J.P., Cotten, J., 2005. Temporal evolution of magmatism in the Northern Volcanic Zone of the Andes: the geology and petrology of Cayambe Volcanic Complex (Ecuador). Journal of Petrology 46, 2225–2252.

Santamaria, F., Schubert, C., 1974. Geochemistry and geochronology of the southern Caribbean–northern Venezuela plate boundary. Geological Society of America Bulletin 85, 1085-1098.

Saunders, J.B., Bernoulli, D., Martin-Kaye, P.H.A. 1985, Late Eocene deep-water clastics in Grenada, West Indies. Eclogae Geologicae Helvetiae, 78, 469–485.

Schärer, U., 1984. The effect of initial ^{230}Th disequilibrium on young UPb ages: the Makalu case, Himalaya. Earth and Planetary Science Letters 67, 191-204.

Schiano, P., Eiler, J.M., Hutcheon, I.D., Stopler, E.M., 2000. Primitive CaO-rich, silica-undersaturated melts in island arcs: Evidence for the involvement of clinopyroxene-rich lithologies in the petrogenesis of arc magmas. Geochemistry, Geophysics, Geosystems 1, doi: 10.1029/1999GC000032.

Scholl, D.W., von Huene, R., 2009. Implications of estimated magmatic additions and recycling losses at the subduction zones of accretionary (non-collisional) and collisional (suturing) orogens. In: Cawood, P. A., Kröner, A. (eds) Earth accretionary systems in space and time.Geological Society, London, Special Publications 318, 105–125.

Sevastianova, I., Clements, B., Hall, R., Belousova, E. A., Griffin, W. L., Pearson, N., 2011. Granitic magmatism, basement ages, and provenance indicators in the Malay Peninsula: insights from detrital zircon U–Pb and Hf-isotope data. Gondwana Research 19, 1024–1039.

Shimizu, N, Arculus, R.J., 1975. Rare earth element concentrations in a suite of basanitoids and alkali olivine basalts from Grenada, Lesser Antilles. Contributions to Mineralogy and Petrology 50, 231-240.

Spandler, C., Pirard, C., 2013. Element recycling from subducting slabs to arc crust: A review. Lithos 170-171, 208-223.

Speed, R. C., Smith-Horowitz, P. L., Perch-Nielsen, K.V.S., Saunders, J. B., Sanfilippo, A. B 1993. Southern Lesser Antilles arc platform: Pre-Late Miocene stratigraphy, structure, and tectonic evolution. Geological Society of America, Special Papers 277, 1-98.

Stamper, C.C., Melekhova, E., Blundy, J.D., Arculus, R.J., Humphreys, C.S., Brooker, R.A., 2014. Oxidized phase relations of a primitive basalt from Grenada, Lesser Antilles. Contributions to Mineralogy and Petrology 167, 954-974

Stern, C.R., 2011. Subduction erosion: Rates, mechanisms, and its role in arc magmatism and the evolution of the continental crust and mantle. Gondwana Research 20, 184-308.

Stern, C.R., Kilian, R., 1996. Role of the subducted slab, mantle wedge and continental crust in the generation of adakites from the Andean Austral volcanic zone. Contributions to Mineralogy and Petrology 123, 263–281.

Sun, S.S., McDonough, W.F., 1989. Chemical and isotopic systematics of oceanic basalts: implications for mantle composition and processes. In Magmatism in the Ocean Basins (eds. A. D. Saunders and M. J. Norry, vol. 42.). The Geological Society, pp. 313–345.

Tang, M., Wang, X.-L., Shu, X.-J., Wang, D., Yang, T., Gopon, P., 2014. Hafnium heterogerneity in zircons from granitic rocks: Geochemical evaluation and modelling of "zircon effect" in crustal anatexis, Earth and Planetary Sciences 389, 188-189.

Théveniaut H., Delor C., Lafon J.M., Monié P., Rossi P., Lahondère D., 2006, Paleoproterozoic (2155-1970 Ma) evolution of the Guiana Shield (Transamazonian event) in the light of new paleomagnetic data from French Guiana. Precambrian Res., 150, 221-256.

Thirlwall, M.F., Graham, A.M., 1984. Evolution of high-Ca, high-Sr series basalts from Grenada, Lesser Antilles: contamination in the arc crust. Journal of the Geological Society, London 141, 427–445.

Thirlwall, M.F., Graham, A.M., Arculus, R.J., Harmon, R.S., Macpherson, C.G., 1996. Resolution of the effects of crustal contamination, sediment subduction, and fluid transport in island arc magmas: Pb–Sr–Nd–O isotope geochemistry of Grenada, Lesser Antilles. Geochimica et Cosmochimica Acta 60, 4785 – 4810.

Torsvik, T.H., Amundsen, H., Hartz, E.H., Corfu, F., Kusznir, N., Gaina, C., Doubrovine, P.V., Steuinberger, B., Ashwal, L.D., Jamtveit, B., 2013. A Precambrian microcontinent in the Indian Ocean. Nature Geoscience 6, 223-227.

Trail, D., Watson, E.B., Tailby, N.D., 2012. Ce and Eu anomalies in zircon as proxies for the oxidation state of magmas. Geochimica et Cosmochimica Acta 97, 70-87.

Turner, S., Hawkesworth, C., van Calsteren, P., Heath, E., Macdonald, R., Black, S., 1996. U-series isotopes and destructive margin magma genesis in the Lesser Antilles: Earth and Planetary Science Letters 142, 191–207.

Turner, S. J., C. H. Langmuir, R. F. Katz, M. A. Dungan, and S. Escrig (2016), Parental arc

magma compositions dominantly controlled by mantle-wedge thermal structure, Nat. Geosci., 9, 772–776.

Vanderhaeghe, O., Ledru, P., Thiéblemeont, D., Egal, E., Cocherie, A., Tegyey, M., Milesi, J.P., 1998. Contrasting mechanism of crustal growth Geodynamic evolution of the granite-greenstone belts of French Guiana. Precambrian Research 85, 1–25.

Van Soest, M.C., Hilton, D.R., Macpherson, C.G., Mattey, D.P., 2002. Resolving sediment subduction and crustal contamination in the Lesser Antilles island arc: A combined He-O-Sr isotope approach: Journal of Petrology 43, 143–170

Vervoort, J.D., Plank, T., Prytulak, J., 2011, The Hf-Nd isotopic composition of marine sediments. Geochimica et Cosmochimica Acta 75, 5903 – 5926.

von Quadt, A., Gallhofer, D., Guillong, M., Peytcheva, I., Waelle, M., Sakata, S., 2014. U–Pb dating of CA/non-CA treated zircons obtained by LA-ICP-MS and CA-TIMS techniques: impact for their geological interpretation. J Anal At Spectrom 29(9):1618–1629.

Weber, J.C., Dixon, T.H., DeMets, C., Ambeh, W.B., Jansma, P., Mattioli, G., Saleh, J., Sella, G., Bilham, R., Pérez, O., 2001. GPS estimate of relative motion between the Caribbean and South American plates, and geologic implications for Trinidad and Venezuela. Geology 29, 75-78.

Westbrook, G. K., Mascle, A., Biju-Duval, B., 1984. Geophysics and structure of the Lesser Antilles forearc. In Biju-Duval, B., Moore, J. C , et al., Initial Reports DSDP, 78A: Washington (U.S. Government. Printing Office), 23-38.

Xie, X., Mann, P., Escalona, A., 2010. Regional provenance study of Eocene clastic sedimentary rocks within the South America-Caribbean plate boundary zone using detrital zircon geochronoloy. Earth and Planetary Science Letters 291, 159–171.

Xie, X., Mann, P., 2014. U–Pb detrital zircon age patterns of Cenozoic clastic sedimentary rocks in Trinidad and its implications. Sedimentary Geology 307, 7-16.

Figure captions: (these captions are too short)

Figure captions

Fig. 1. Regional bathymetric map of the Lesser Antilles arc showing: a) position of the inner (younger) and outer (older) arcs as well as the Aves ridges, the Grenada and Tobago basins, b) Location of the Orinoco River and the Orinoco River delta south of the Lesser Antilles arc. Inset shows location of Fig. 2.

Fig. 2. Geological map of Grenada after (Legend 1&2) Arculus (1976), Saunders et al. (1985) and (Legend 3) Robertson (2005). The geological map of Carriacou after Donovan et al. (2003). The location of Petite Martinique relative to Carriacou is also shown.

Fig. 3. Concordia diagrams showing SHRIMP analytical data from Canberra (a, b) and Beijing (c, d, e, f) for samples from Grenada, Carriacou and Petite Martinique.

Fig. 4. Concordia diagrams showing LA-ICP-MS results from Mainz (a, f, g) and London (b, e) and SHRIMP data (c, d) for zircons from samples from Grenada, Carriacou and Petite Martinique. **Fig. 5.** Concordia diagrams showing SHRIMP (a) and LA-ICP-MS (c, d) data for zircons of samples from Grenada and Carriacou.

Fig. 6. Total alkali versus silica (TAS) classification diagram (LeBas et al., 1986) for samples from Grenada, Carriacou and Petite Martinique. Samples with black spot or black cross inside indicate samples containing zircon.

Fig. 7. Chondrite-normalized REE patterns of studied samples (a, c, e). Normalizing values from McDonough and Sun (1995). (b, d, f) Multi-element variation diagrams normalized to N-MORB (Sun and McDonough, 1989).

Fig. 8. $^{87}Sr/^{86}Sr$ vs. $^{144}Nd/^{143}Nd$ diagram. Data for MORB are from Hart et al. (1999) and Kelemen et al. (2003); Cretaceous Atlantic MORB data are from (Jahn et al., 1980); the adakite field includes data from Ecuador (Samaniego et al., 2005), Chile (Stern and Kilian, 1996), Argentina (Kay et al., 1993), Mexico (Aguillón-Robles et al., 2001), and Panama-Costa Rica (Defant et al., 1992); the Antilles Sediments and Sediments subducted at trenches fields are from Plank and Langmuir (1998); and the Atlantic Cretaceous Pelagic Sediment (AKPS) field was constructed after data from (Jolly et al., 2006). Mixing curve between NMORB (Hart et al., 1999) and South Antilles Terrigene Sediment is from Plank and Langmuir (1998).

Fig. 9. Representative cathodoluminiescence images (CL) for young igneous (a,b,c) and xenocristiczircons (d). Numbers above CL images in a, b, c indicate mean age for the sample. Numbers in d show single spot ages. SHRIMP spot sites are shown together (in some cases) with laser ablation sites for isotopic trace elements and Hf isotopic analysis. Scale bars are all 100 µm.

Fig. 10. Hf isotope evolution diagrams for zircons from Grenada samples. Note spread in $\varepsilon_{Hf(t)}$ values (a, b) suggesting a heterogeneous source.

Fig. 11. Rare earth element concentration in zircons representing the Recent (a, b) and the Older Arc (c, d) as well as xenocristiczircons (e).

Fig. 12. Paleogeographic reconstruction showing the effects of interaction between northern South America and the Greater Antilles arc, modified after Escalona and Mann (2006); Xie et al (2010); Xie and Mann (2014). The inferred paths of major paleofluvial systems (Maracaibo and Orinoco rivers) draining from northern South America is shown from the: a) Early Eocene (~50 Ma); b) Middle Oligocene (~30 Ma); c) Middle Miocene (~14 Ma); and d) Pliocene (~5 Ma). See text for discussion (section 5.4).

Table captions

Table 1a. SHRIMP II analytical data (Beijing SHRIMP Center) for spot analyses of single zircons from Grenada rocks, using the SQUID data reduction procedure. In bold best ages.

Table 1b. SHRIMP II analytical data (Beijing SHRIMP Center) for spot analyses of magmatic zircons from rocks of the Grenadine Islands, using the Nelson (1997) data reduction procedure.

Table 2. SHRIMP analytical results for zircons >2 Ma obtained at the Beijing SHRIMP Center.

Table 3. SHRIMP analytical results for zircons <2 Ma obtained at the Research School of Earth Sciences, Australian National University, Canberra.

Table 4. LA-ICP-MS analyses of zircons from Grenada, Carriacou and Petite Martinique islands (measured at the Natural History Museum, London, and Mainz University), using an in house data reduction procedure. In bold best ages.

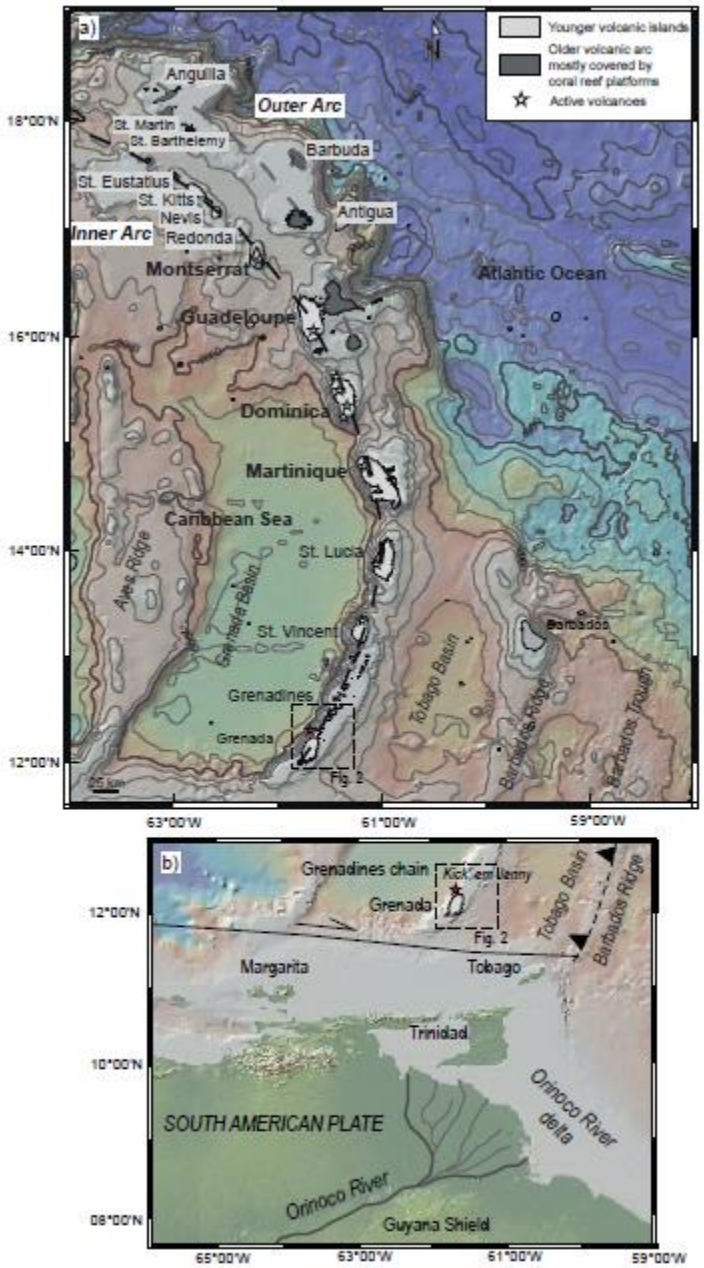

Fig. 1
Rojas-Agramonte et al.

Figure 1

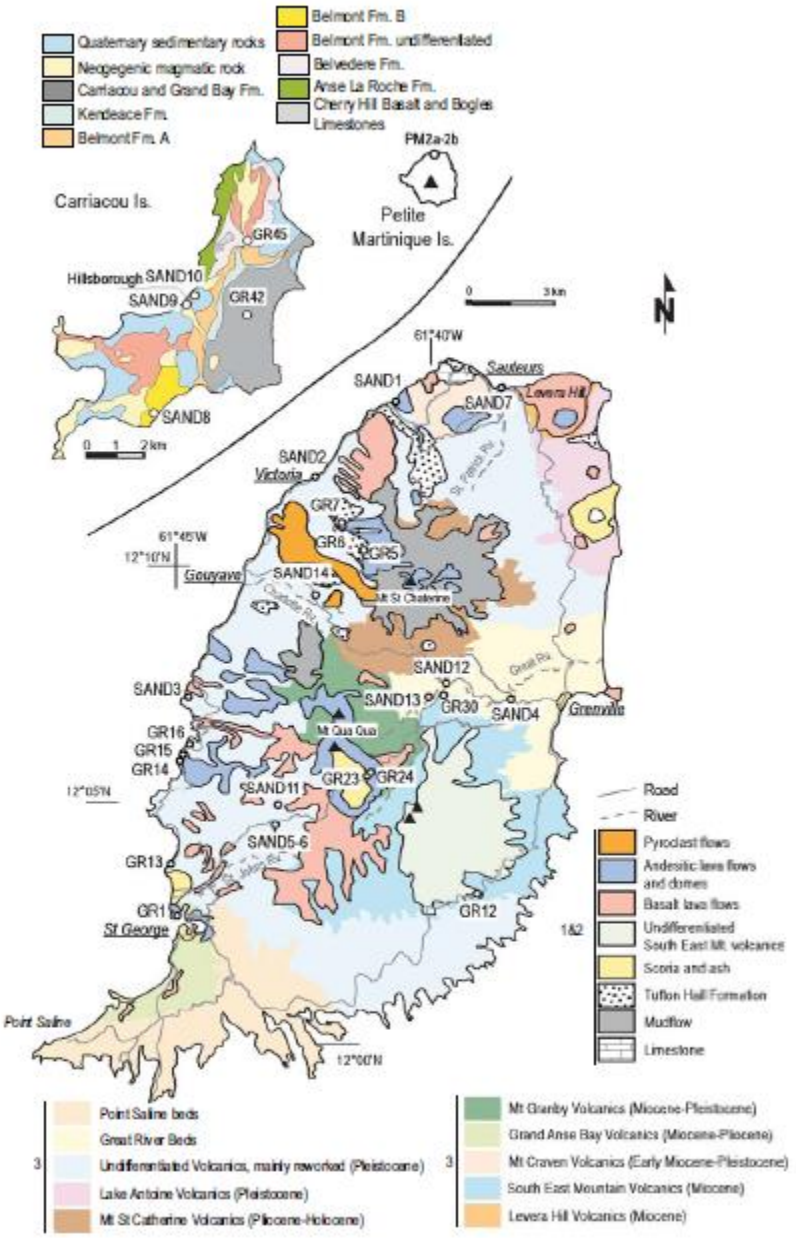

Fig. 2
Rojas-Agramonte et al.,

Figure 2

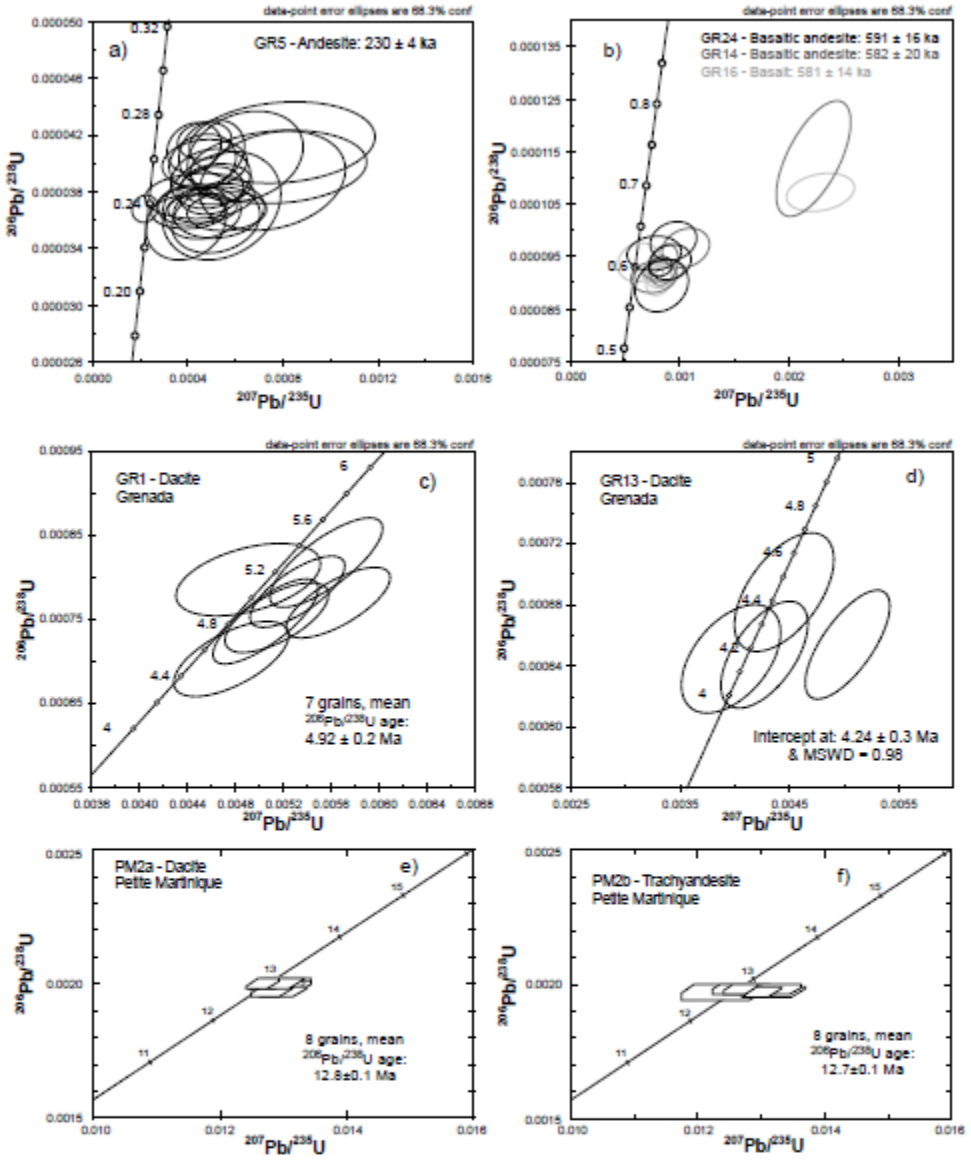

Fig. 3
Rojas-Agramonte et al.,

Figure 3

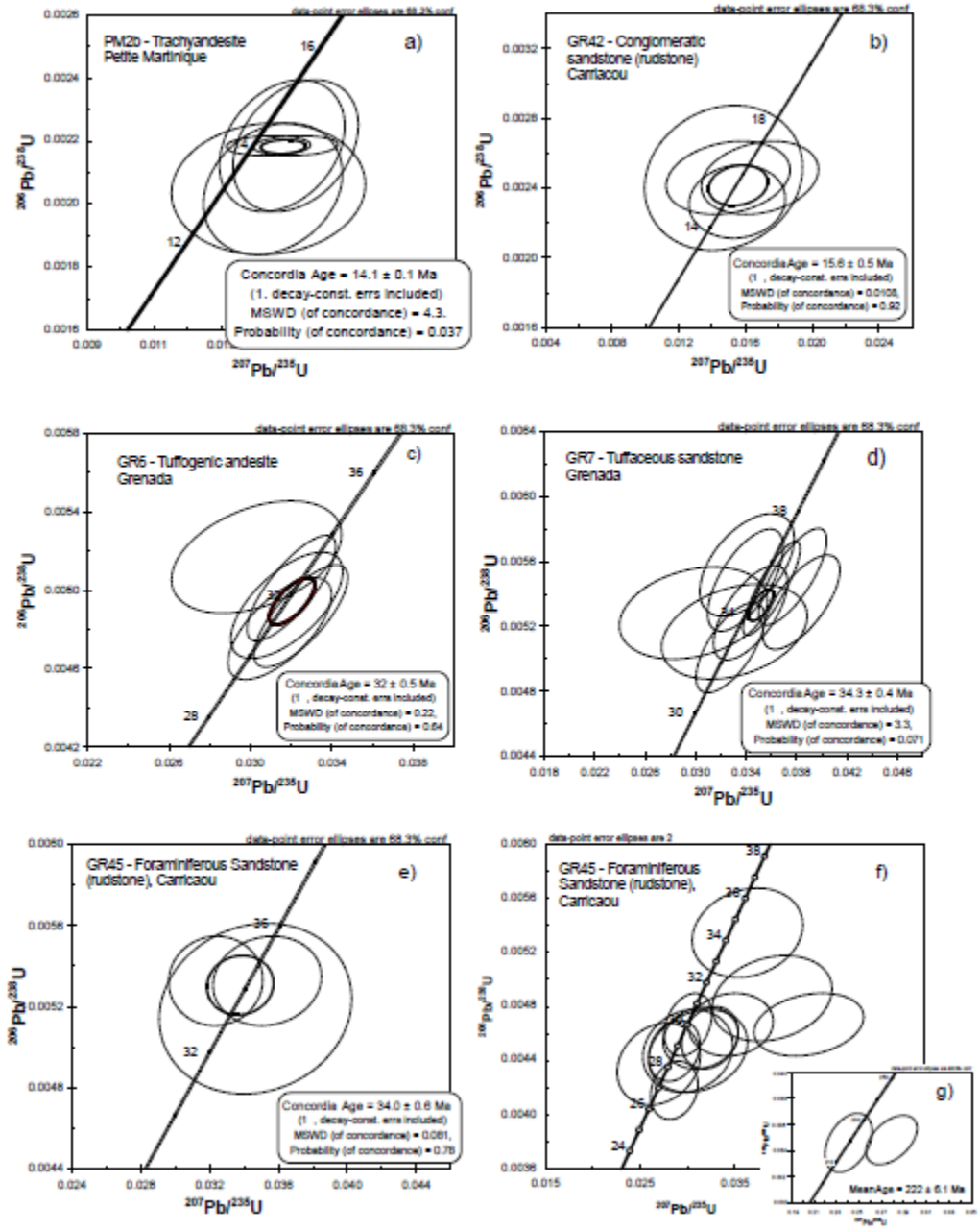

Fig. 4
Rojas-Agramonte et al.,

Figure 4

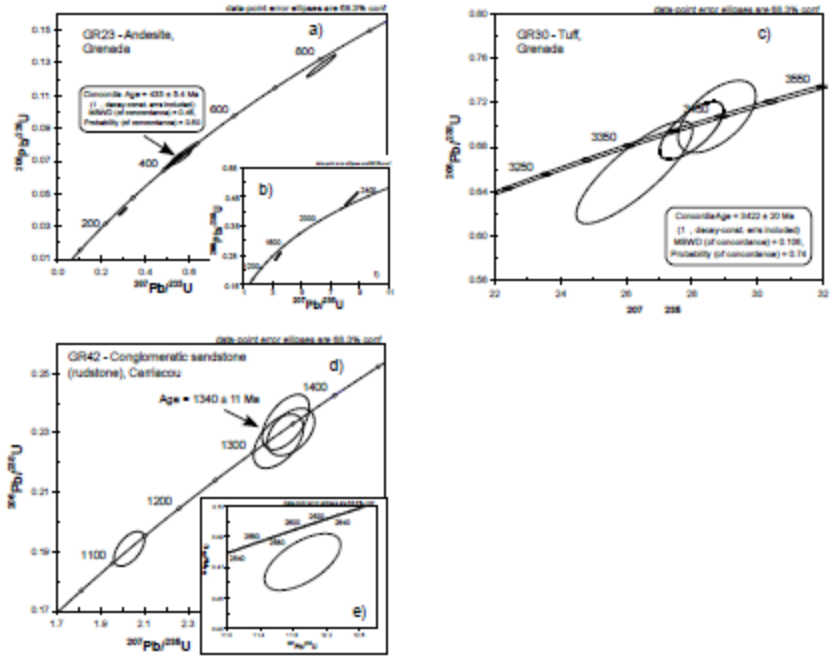

Fig. 5
Rojas-Agramonte et al.,

Figure 5

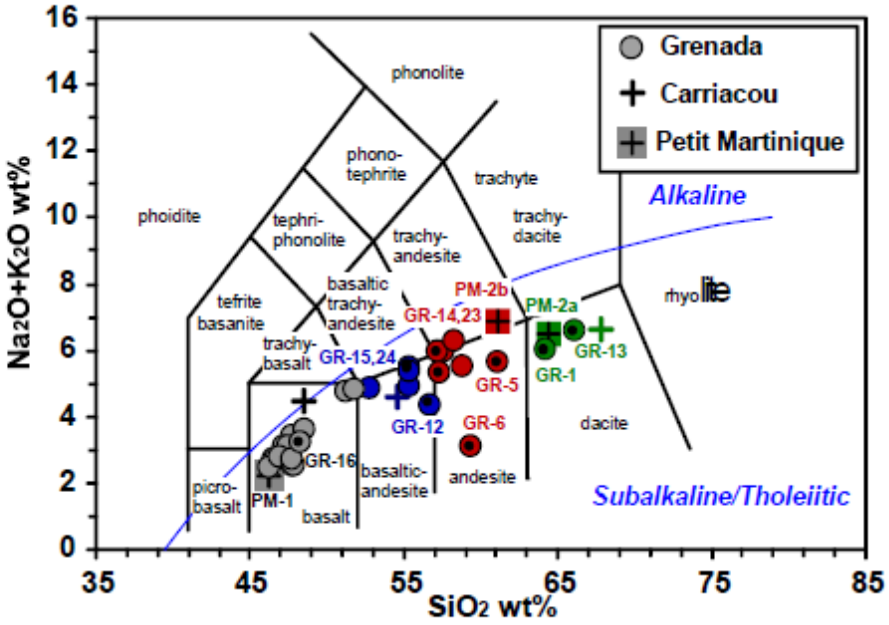

Fig. 6
Rojas-Agramonte et al.

Figure 6

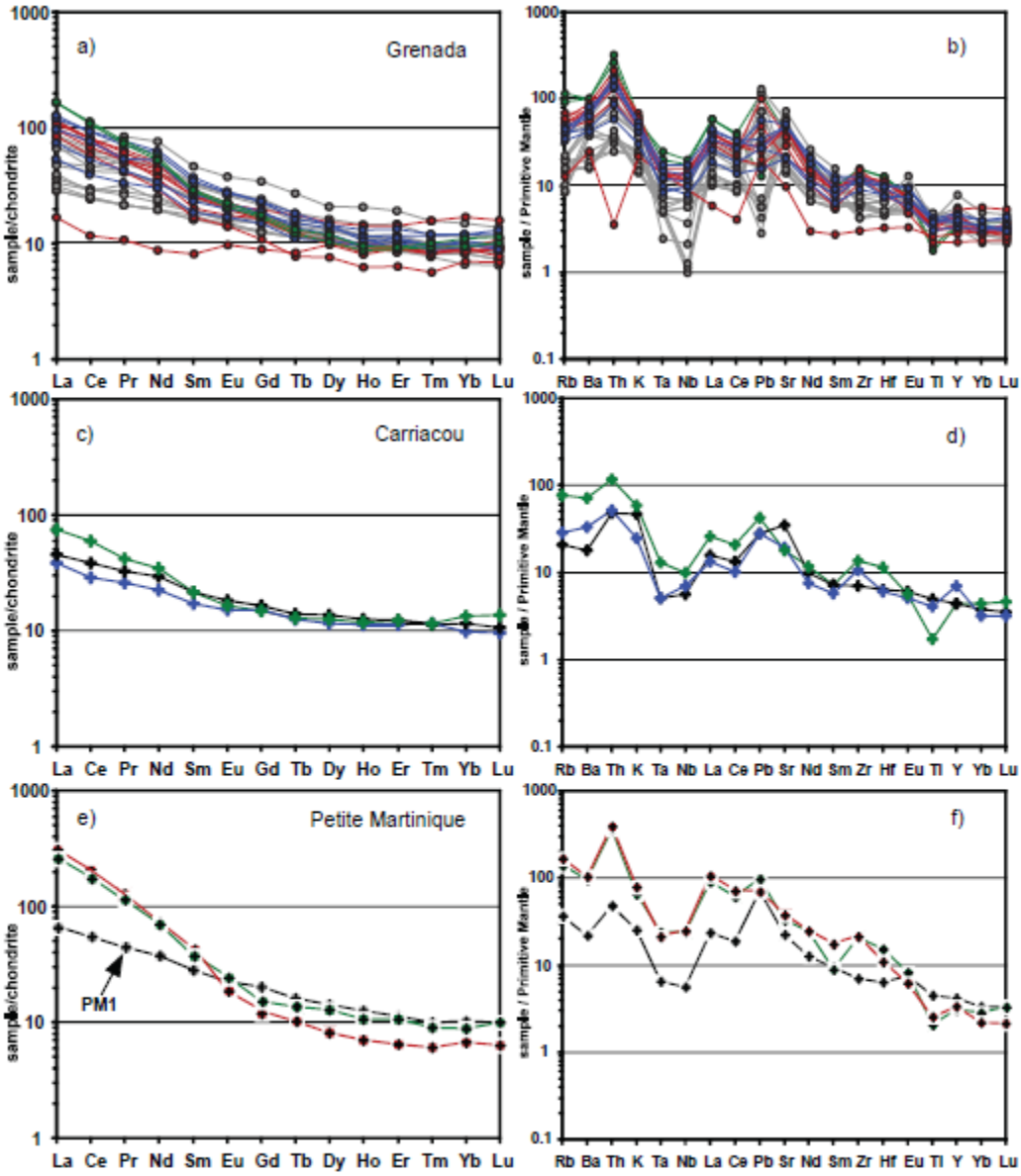

Fig. 7
Rojas-Agramonte et al.

Figure 7

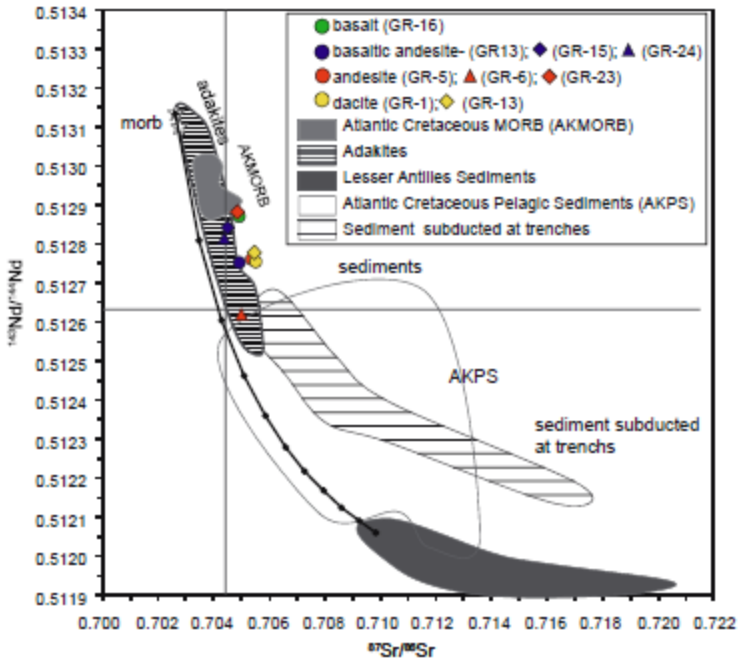

Fig. 8
Rojas-Agramonte et al.,

Figure 8

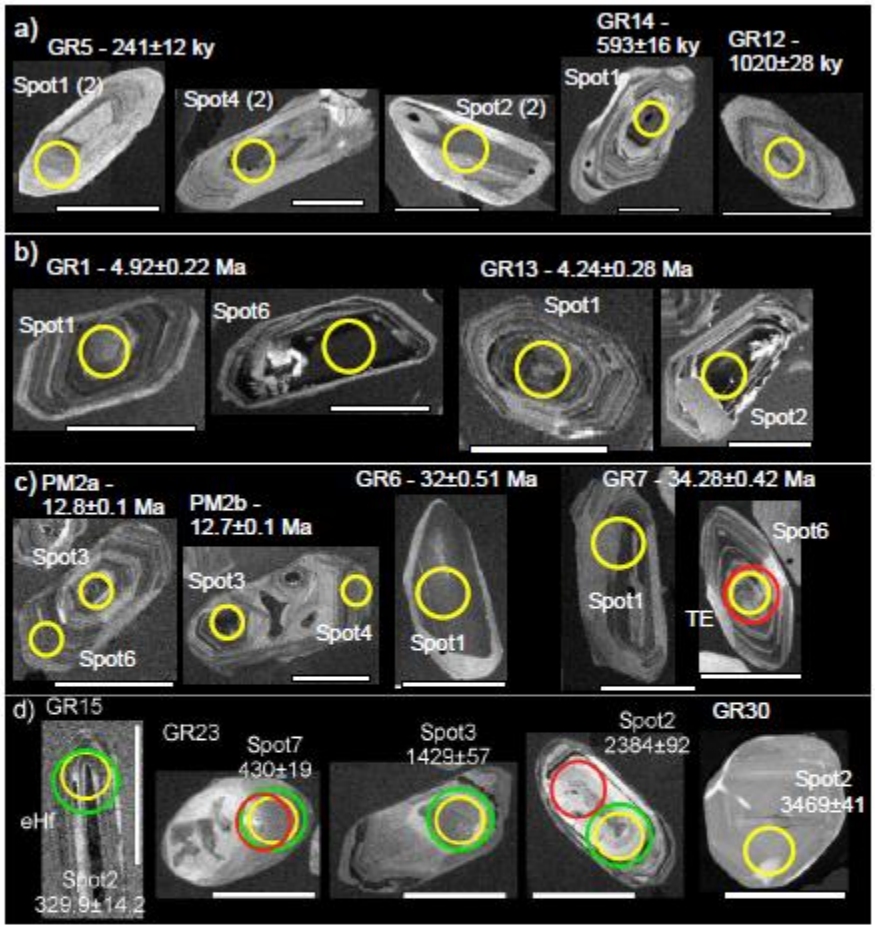

Fig. 9
Rojas-Agramonte et al.

Figure 9

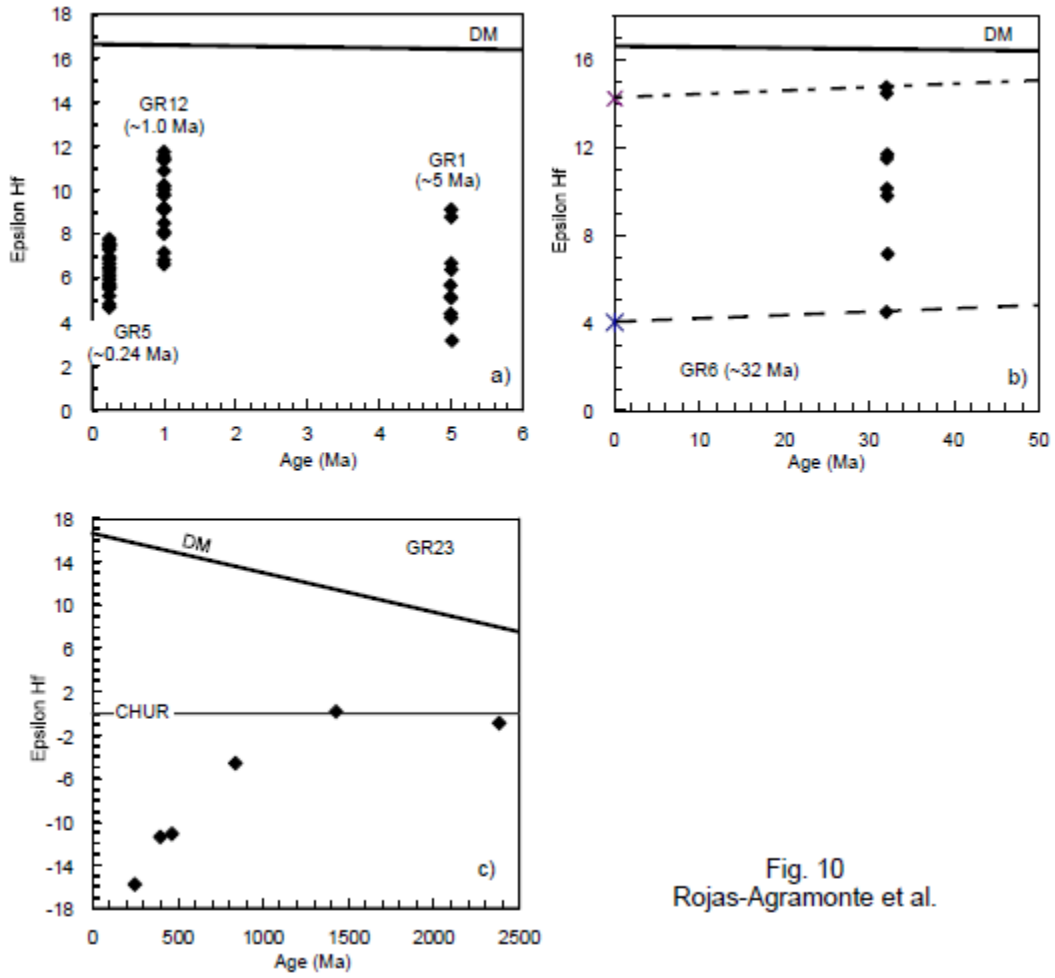

Fig. 10
Rojas-Agramonte et al.

Figure 10

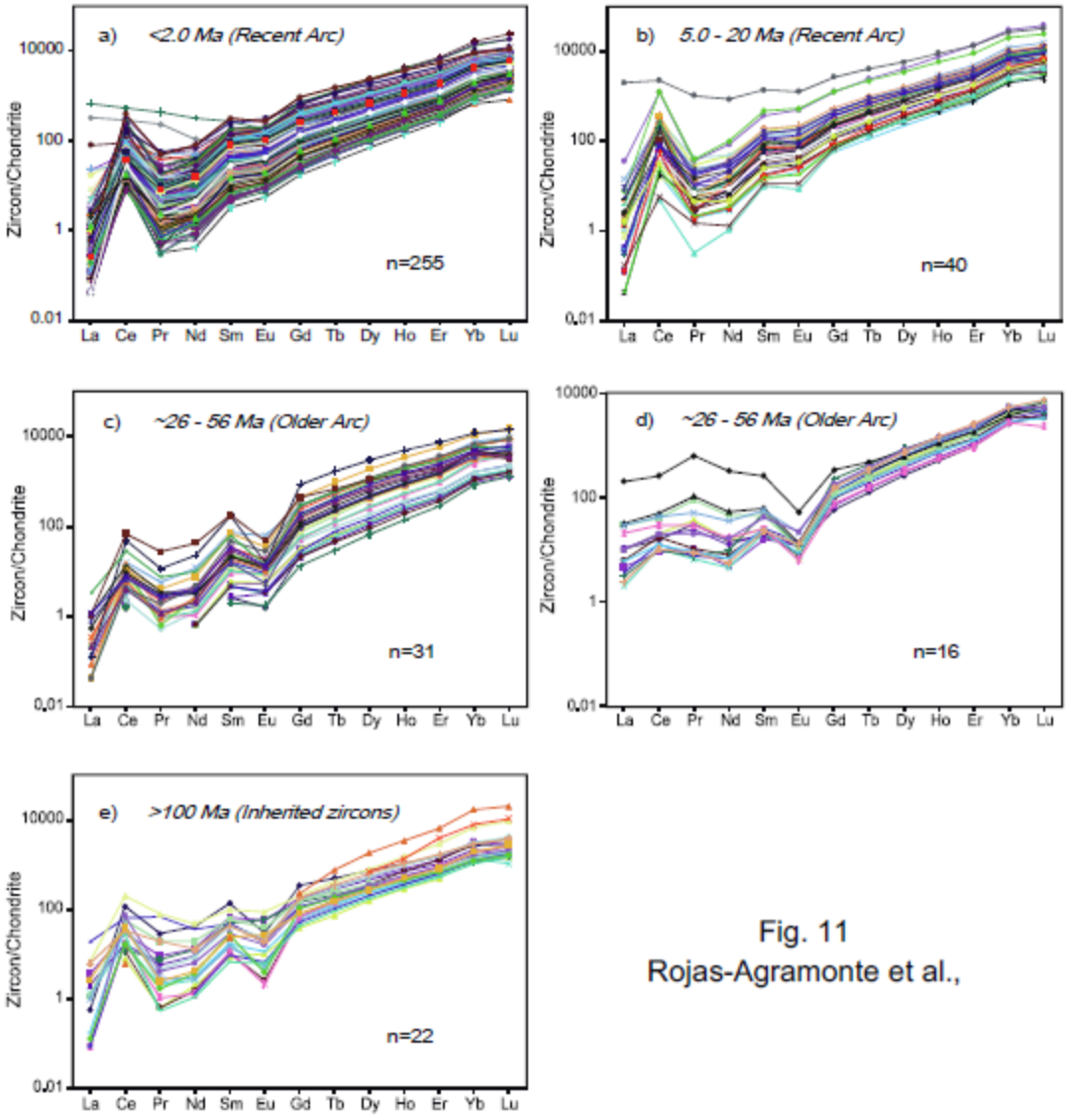

Fig. 11
Rojas-Agramonte et al.,

Figure 11

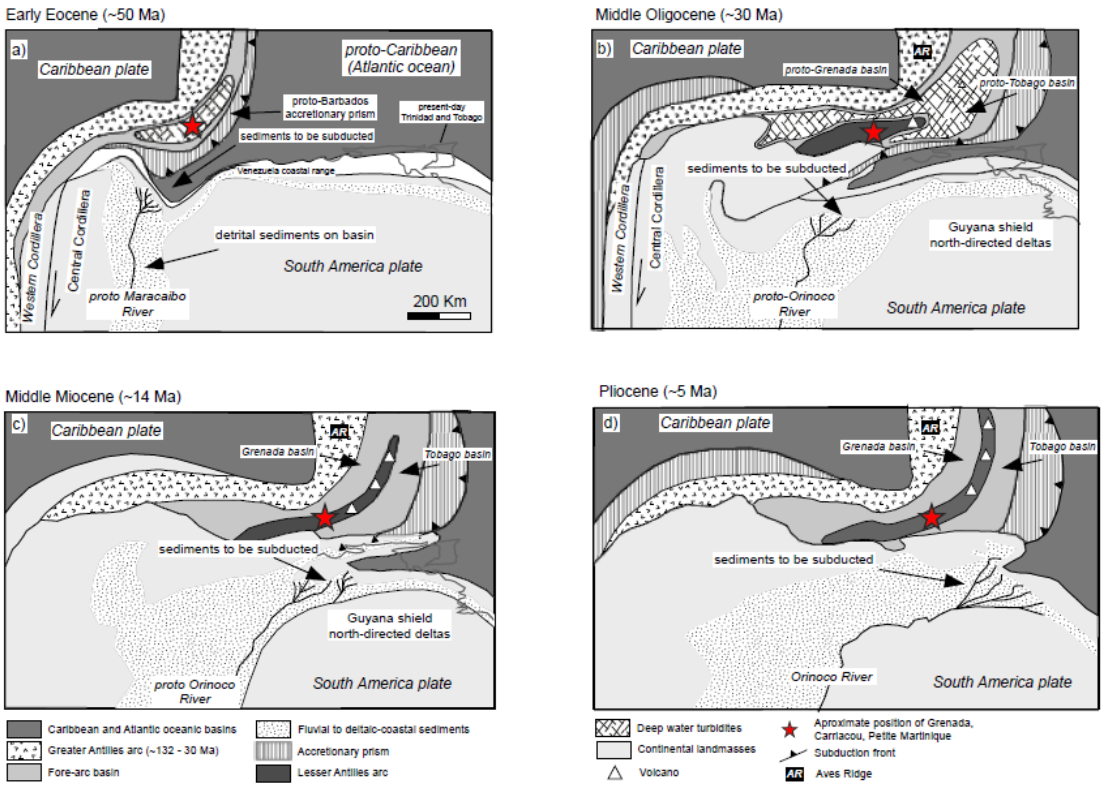

Fig. 12
Rojas-Agramonte et al.,

Figure 12

Table 1a. SHRIMP II analytical data (Beijing SHRIMP center) for spot analyses of single zircons from Grenada rocks, using the SQ
In bold best ages.

Spot	% $^{206}Pb_c$	U (ppm)	Th (ppm)	$^{232}Th/^{238}U$	ppm $^{206}Pb^*$	Total $^{238}U/^{206}Pb$	±%	Total $^{207}Pb/^{206}Pb$	±%	$^{207}Pb^*/^{235}U$	±%	$^{206}Pb^*/^{238}U$
GR1												
GR1-1	0.00	2546	914	0.37	1.54	1,422	4.2	0.0491	5.2	0.00476	6.7	0.000703
GR1-2	0.00	3905	1193	0.32	2.58	1,298	3.6	0.0533	3.6	0.00566	5.1	0.000770
GR1-3	0.46	6206	2280	0.38	4.20	1,271	3.6	0.0529	3.0	0.00532	4.9	0.000783
GR1-4	0.20	6050	4550	0.78	4.26	1,220	4.3	0.0508	2.8	0.00556	5.6	0.000818
GR1-5	0.21	7297	9210	1.30	4.70	1,334	4.5	0.0506	2.8	0.00505	5.8	0.000748
GR1-6	0.26	7200	8144	1.17	4.95	1,250	3.6	0.0466	6.2	0.00491	8.1	0.000798
GR1-7	0.26	5926	1963	0.34	3.84	1,325	3.6	0.0516	3.1	0.00515	5.6	0.000753
GR6												
GR6-1	0.00	441	40	0.09	1.83	207.4	3.7	0.0593	4.2	0.0394	5.5	0.00482
GR6-2	0.00	1705	332	0.20	7.13	205.4	3.5	0.0484	3.1	0.0325	4.7	0.00487
GR6-3	0.00	1272	227	0.18	5.47	199.6	3.5	0.0463	2.8	0.0320	4.5	0.00501
GR6-4	0.25	1069	181	0.17	4.42	207.6	3.6	0.0495	3.1	0.0314	5.3	0.00480
~~GR6-5~~	~~0.51~~	~~506~~	~~74~~	~~0.15~~	~~2.26~~	~~192.5~~	~~3.6~~	~~0.0466~~	~~3.8~~	~~0.0303~~	~~9.1~~	~~0.00517~~
GR6-6	0.00	518	57	0.11	2.19	203.1	3.6	0.0468	4.4	0.0318	5.7	0.00492
~~GR6-7~~	~~0.00~~	~~788~~	~~417~~	~~0.55~~	~~0.0400~~	~~16,900~~	~~8.0~~	~~0.726~~	~~11~~	~~0.00592~~	~~14~~	~~0.0000592~~
GR7												
GR7-1	0.39	500	73	0.15	2.40	178.5	3.7	0.0474	4.0	0.0341	7.2	0.00558
GR7-2	0.70	423	43	0.10	1.89	192.1	3.7	0.0520	5.9	0.0331	12	0.00517
GR7-3	0.00	390	49	0.13	1.84	182.3	3.8	0.0449	4.4	0.0340	5.8	0.00549
GR7-4	0.00	679	81	0.12	3.12	186.9	3.6	0.0520	3.8	0.0384	5.3	0.00535
GR7-5	0.00	773	42	0.06	3.66	181.6	3.6	0.0496	3.1	0.0377	4.7	0.00551
GR7-6	0.00	1690	231	0.14	7.89	184.0	3.5	0.0481	2.2	0.0360	4.1	0.00544
GR7-7	0.00	553	39	0.07	2.51	189.2	3.6	0.0472	4.3	0.0344	5.6	0.00528
~~GR7-8~~	~~0.00~~	~~751~~	~~81~~	~~0.11~~	~~3.96~~	~~163.2~~	~~3.6~~	~~0.9631~~	~~1.0~~	~~0.814~~	~~3.7~~	~~0.00613~~
GR7-9	0.00	1147	362	0.33	5.20	189.3	3.5	0.0410	12	0.0298	13	0.00528
GR7-10	0.00	440	31	0.07	1.91	197.3	3.6	0.0469	4.1	0.0328	5.5	0.00507
GR13												
GR13-1	0.00	4321	1856	0.44	2.43	1,529	3.6	0.0558	3.6	0.00503	5.1	0.000654
GR13-2	0.32	6033	4974	0.85	3.37	1,540	3.6	0.0504	3.0	0.00427	6.2	0.000647
GR13-3	0.41	3581	1632	0.47	1.99	1,545	3.6	0.0479	4.3	0.00396	7.6	0.000645
GR13-4	0.00	3801	1568	0.43	2.25	1,453	3.7	0.0469	5.6	0.00445	6.7	0.000688
~~GR13-5~~	~~1.62~~	~~2213~~	~~919~~	~~0.43~~	~~1.56~~	~~1,217~~	~~7.5~~	~~0.33~~	~~51~~	~~0.036~~	~~53~~	~~0.000808~~

Table 1a. Continue

Spot	% $^{206}Pb_c$	U (ppm)	Th (ppm)	$^{232}Th/^{238}U$	ppm $^{206}Pb^*$	Total $^{238}U/^{206}Pb$	±%	Total $^{207}Pb/^{206}Pb$	±%	$^{207}Pb^*/^{235}U$	±%	$^{206}Pb^*/^{238}U$
GR13												
~~GR13-~~	~~0.00~~	~~4752~~	~~2764~~	~~0.60~~	~~2.36~~	~~1,732~~	~~4.1~~	~~0.0459~~	~~4.0~~	~~0.00365~~		~~0.000578~~

~~6~~											~~5.7~~	
~~GR13-7~~	~~0.00~~	~~5409~~	~~4696~~	~~0.90~~	~~3.65~~	~~1,272~~	~~3.6~~	~~1.347~~	~~1.0~~	~~0.1459~~	~~3.7~~	~~0.000786~~
~~GR13-8~~	~~0.00~~	~~9741~~	~~11016~~	~~1.17~~	~~5.20~~	~~1,610~~	~~3.5~~	~~1.753~~	~~0.79~~	~~0.1501~~	~~3.6~~	~~0.000621~~
GR15												
GR15-2	1.07	1597	783	0.51	91.0	15.08	3.5	0.2303	0.55	2.022	3.6	0.0656
GR16												
GR16-3	0.04	321	167	0.54	38.2	7.22	3.5	0.07205	1.1	1.368	3.7	0.1384
GR23												
GR23-2	0.01	212	91	0.44	80.3	2.267	3.5	0.13940	0.45	8.47	3.6	0.441
GR23-3	0.02	589	82	0.14	124	4.08	3.5	0.10074	0.42	3.40	3.5	0.2453
GR23-4	0.04	533	224	0.43	58.8	7.79	3.5	0.06846	0.71	1.205	3.6	0.1283
GR23-5	0.00	577	109	0.20	36.6	13.56	3.5	0.05585	1.0	0.568	3.7	0.0737
GR23-6	0.01	2128	75	0.04	125	14.61	3.5	0.05518	0.48	0.520	3.6	0.0684
GR23-7	0.03	2259	202	0.09	132	14.69	3.5	0.05591	0.56	0.523	3.6	0.0680
GR23-8	0.08	2241	99	0.05	75.4	25.54	3.5	0.05563	1.1	0.297	3.7	0.0391
GR23-9	0.19	305	55	0.19	18.7	14.04	3.5	0.05762	1.4	0.550	4.1	0.0711

Table 1b. SHRIMP II analytical data (Beijing SHRIMP center) for spot analyses on magmatic zircons from rocks of the Grenadine Islands, using the Nelson (1997) data reduction procedure.

Sample No.	U ppm	Th ppm	206Pb/204Pb	207Pb/206Pb	206Pb/238U	207Pb/235U	206/238 age ± 1s	207/235 age ± 1s	207/206 age ± 1s
PM2a									
PM2a-1	2587	1801	16864	0.0478±11	0.00197±3	0.01301±36	13±0.	13±0.	89±55
PM2a-2	1750	562	12225	0.0471±15	0.00200±3	0.01299±46	13±0	13±0	53±63
PM2a-3	3158	2143	22523	0.0463± 9	0.00200±3	0.01277±30	13±0	13±0	12±28
PM2a-4	2118	851	13755	0.0471±13	0.00199±3	0.01292±42	13±0	13±0	53±59
PM2a-5	1879	804	12255	0.0473±15	0.00199±3	0.01230±45	13±	13±	66±69
PM2a-6	4338	2170	27933	0.0460± 7	0.00200±3	0.01268±27	13±	13±	0±17
PM2a-7	2847	1130	18727	0.0471±10	0.00198±3	0.01283±34	13±	13±	55±51
PM2a-8	3593	2242	25316	0.0472± 8	0.00201±3	0.01305±29	13±	13±	57±40
PM2b									
PM2b-1	1648	753	10776	0.0485±16	0.00198±3	0.01321±50	13±0.	13±0.	122±80
PM2b-2	314	123	17271	0.0456±23	0.00197±3	0.01242±68	13±0	13±0	0±48
PM2b-3	4375	6487	16181	0.0464± 8	0.00198±2	0.01260±29	13±0	13±0	18±30
PM2b-4	2081	931	14684	0.0485±13	0.00198±3	0.01325±40	13±0	13±0	125±61
PM2b-5	3208	1399	23202	0.0479± 8	0.00198±3	0.01304±30	13±0.	13±	94±42
PM2b-6	1805	889	12225	0.0463±15	0.00199±3	0.01269±45	13±0.	13±	12±43

Table 2. SHRIMP zircon U–Pb analytical results (> 2 Ma) obtained at the Beijing SHRIMP center. In Italic values excluded from the mean age calculation because are too young or too old.

					Total Pb, before common Pb correction									Corrected for disequilibrium			Mean	
	Pb	U	Th		204Pb			208Pb		207Pb		206Pb		206Pb*	and initial 234U and 230Th			sample	95%
Sample	ppb	ppm	ppm	Th/U	206Pb	±	f206(%)	206Pb	±	206Pb	±	238U	±	238U	206Pb*/ 238U	Date (ka)	±	age (ka)	c.l.
GR5																			
GR5-1	15	2547	1431	0.5805	-	-	0.134	0.422	13.6	0.1638	20.7	2.53E-05	2.11E-06	2.58E-05	3.773E-05	243	14		
GR5-2	31	2162	1902	0.9090	-	-	0.283	0.760	13.4	0.2909	12.7	2.34E-05	2.38E-06	2.43E-05	3.405E-05	220	15		
GR5-3	31	2184	2025	0.9577	-	-	0.283	0.669	11.8	0.2903	10.5	2.77E-05	2.44E-06	2.88E-05	3.856E-05	249	16		
GR5-2.1	54	282	88	0.3227	7.05E-02	8.11E+01	0.501	1.610	8.358	0.4755	8.8	2.61E-05	3.23E-06	2.86E-05	4.243E-05	274	21		
GR5-3.1	47	466	244	0.5414	5.20E-02	3.70E+03	0.435	1.373	7.030	0.4199	8.1	2.77E-05	2.48E-06	2.97E-05	4.220E-05	272	16		
GR5-4.1	78	854	574	0.6945	4.54E-02	2.54E+01	0.716	1.754	2.787	0.6584	2.4	2.91E-05	3.86E-06	3.69E-05	4.880E-05	*315*	25		
GR5-5.1	21	2276	1865	0.8469	4.53E-02	4.81E+01	0.188	0.690	5.767	0.2094	5.6	2.44E-05	8.29E-07	2.50E-05	3.519E-05	227	5		
GR5-6.1	48	588	326	0.5735	5.13E-02	1.05E+02	0.440	1.304	6.396	0.4237	6.3	3.06E-05	2.25E-06	3.29E-05	4.543E-05	293	15		
GR5-7.1	87	3100	171	0.5693	3.69E-02	6.11E+01	0.807	1.958	4.351	0.7357	3.0	3.23E-05	7.70E-06	4.93E-05	6.241E-05	*402*	50		
GR5-8.1	30	1675	1229	0.7581	3.41E-02	3.56E+01	0.271	0.874	4.228	0.2804	3.9	3.98E-05	1.34E-06	4.13E-05	5.293E-05	*341*	9		
GR5-9.1	41	3200	3117	1.0064	2.93E-02	2.26E+01	0.375	1.064	3.537	0.3688	5.8	3.07E-05	1.63E-06	3.25E-05	4.216E-05	272	11	245	13
GR5-10.1	30	1366	936	0.7080	2.83E-02	9.20E+01	0.271	0.842	5.468	0.2800	5.1	2.86E-05	1.21E-06	2.97E-05	4.112E-05	265	8		
GR5-11.1	22	1497	678	0.4684	2.97E-02	4.14E+01	0.197	0.679	7.359	0.2173	7.3	2.13E-05	8.51E-07	2.18E-05	3.406E-05	220	5		
GR5-1	36	1600	1023	0.6606	-7.18E-02	6.35E+01	0.326	0.733	9.281	0.3269	9.9	2.73E-05	2.16E-06	2.86E-05	4.027E-05	260	14		
GR5-2	14	2769	4220	1.5747	-	-	0.124	0.682	7.125	0.1557	11.3	2.76E-05	1.33E-06	2.81E-05	3.396E-05	219	9		
GR5-3	25	932	613	0.6798	-1.53E-	6.38E+01	0.228	0.730	11.955	0.2440	16.5	2.86E-05	2.67E-06	2.94E-05	4.101E-05	264	17		

					01														
GR 5-4	25	2160	2055	0.9833	-	-	0.227	0.882	7.000	0.2427	13.5	2.64E-05	1.84E-06	2.72E-05	3.671E-05	237	12		
GR 5-5	37	11120	729	0.6722	-1.06E-01	6.46E+01	0.335	0.794	9.840	0.3346	11.8	2.42E-05	2.32E-06	2.53E-05	3.664E-05	236	15		
GR 5-6	11	15266	874	0.5917	-8.47E-02	6.44E+01	0.097	0.600	9.692	0.1329	28.4	2.93E-05	2.14E-06	2.97E-05	4.188E-05	270	14		
GR 5-7	26	36788	5331	1.4975	-4.44E-02	6.50E+01	0.238	0.795	6.748	0.2523	18.7	2.68E-05	2.45E-06	2.77E-05	3.400E-05	219	16		
GR 5-8	11	29900	3457	1.1946	-4.75E-02	6.47E+01	0.097	0.608	15.400	0.1320	11.9	2.78E-05	1.26E-06	2.82E-05	3.645E-05	235	8		
GR 5-9	17	20566	1642	0.8255	-	-	0.149	0.686	11.168	0.1771	13.3	2.29E-05	1.37E-06	2.34E-05	3.350E-05	216	9		
GR 5-10	24	25005	2311	0.9535	-5.80E-02	3.79E+01	0.214	0.711	7.732	0.2321	10.8	2.17E-05	1.31E-06	2.23E-05	3.155E-05	203	8		
GR 5-11	27	13677	1015	0.7672	-	-	0.248	0.699	9.601	0.2606	12.5	2.46E-05	1.90E-06	2.55E-05	3.617E-05	233	12		
GR 5-12	65	17311	1171	0.6992	-2.35E-02	5.01E+01	0.602	1.430	4.802	0.5619	5.9	2.67E-05	3.41E-06	3.07E-05	4.222E-05	272	22		
GR12																			
GR-12-1	3	18633	1268	0.7034	-5.46E-03	7.09E+01	0.027	0.344	7.520	0.0733	8.4	1.60E-04	8.18E-06	1.61E-04	1.729E-04	*1114*	53		
GR-12-2	2	41788	8826	2.1827	-1.48E-03	4.24E+01	0.016	0.704	3.626	0.0638	8.9	1.67E-04	9.40E-06	1.68E-04	1.667E-04	1075	61		
GR-12-3	5	16244	2641	1.6803	-	-	0.041	0.516	6.555	0.0850	12.0	1.55E-04	8.16E-06	1.56E-04	1.595E-04	1029	53		
GR-12-4	3	14922	636	0.4403	-	-	0.021	0.150	13.112	0.0682	11.7	1.35E-04	8.40E-06	1.36E-04	1.495E-04	964	54		
GR 12.1	7	15911	1117	0.7250	1.22E-02	7.17E+01	0.283	0.386	4.419	0.1019	11.7	1.51E-04	4.66E-06	2.88E-05	1.642E-04	1059	30		
GR 12.2.1	54	4099	159	0.4010	3.89E-02	3.00E+01	0.134	1.242	4.646	0.4724	2.9	1.49E-04	7.15E-06	2.58E-05	1.773E-04	*1143*	46		
GR 12.3.1	15	8575	515	0.6211	1.62E-02	1.20E+02	0.283	0.522	5.657	0.1671	9.4	1.48E-04	4.70E-06	2.43E-05	1.626E-04	1048	30	1034	34
GR 12.4.1	3	15722	1430	0.9394	4.99E-03	1.29E+02	0.283	0.373	3.990	0.0715	6.8	1.53E-04	3.18E-06	2.88E-05	1.639E-04	1057	21		
GR 12.5.1	4	18277	1280	0.7237	7.68E-03	5.19E+01	0.134	0.332	3.813	0.0743	4.1	1.50E-04	3.00E-06	2.58E-05	1.626E-04	1049	19		

GR 12.6 .1	10	460	149	0.3348	4.09E-02	5.12E+01	0.283	0.333	11.557	0.1238	7.2	1.42E-04	3.75E-06	2.43E-05	1.586E-04	1023	24		
GR 12.7 .1	13	483	239	0.5116	2.47E-02	7.54E+01	0.283	0.480	6.189	0.1518	6.1	1.44E-04	3.80E-06	2.88E-05	1.593E-04	1027	24		
GR 12.8 .1	6	1143	808	0.7300	1.49E-02	5.65E+01	0.134	0.358	4.860	0.0929	6.5	1.44E-04	3.44E-06	2.58E-05	1.569E-04	1012	22		
GR14																			
GR 14-1	46	2820	3324	1.2179	-3.05E-03	6.97E+01	0.419	1.095	5.135	0.4065	7.2	7.82E-05	6.66E-06	8.35E-05	9.209E-05	594	43		
GR 14-2	17	3603	4139	1.1869	-4.17E-03	1.41E+02	0.150	0.656	6.483	0.1773	14.1	7.38E-05	4.74E-06	7.53E-05	8.408E-05	542	31		
GR 14-3	19	1473	974	0.6831	-	-	0.172	0.609	11.333	0.1963	16.2	7.94E-05	6.17E-06	8.12E-05	9.353E-05	603	40		
GR 14.1 .1	10	1926	1398	0.7498	1.51E-02	4.73E+01	0.086	0.451	4.456	0.1233	5.4	7.91E-05	2.08E-06	8.02E-05	9.205E-05	593	13	584	24
GR 14.2 .1	18	6501	341	0.5416	4.87E-02	4.93E+01	0.159	0.569	6.778	0.1848	6.3	7.45E-05	2.25E-06	7.60E-05	8.940E-05	576	15		
GR 14.3 .1	9	1639	1620	1.0212	1.26E-02	1.03E+02	0.081	0.518	7.002	0.1189	7.9	7.797 96E-05	1.92E-06	7.89E-05	8.892E-05	573	12		
GR 14.4 .1	34	2448	2130	0.8989	3.06E-02	1.61E+01	0.308	0.925	2.615	0.3114	5.9	8.27E-05	3.60E-06	8.62E-05	9.707E-05	626	23		
GR 14.5 .1	10	702	304	0.4480	2.97E-02	2.26E+02	0.087	0.420	8.837	0.1242	9.6	7.31E-05	2.29E-06	7.41E-05	8.810E-05	568	15		
GR15																			
GR 15-1	10	4265	5103	1.2364	-5.32E-03	5.16E+01	0.085	0.588	7.021	0.1222	8.5	8.40E-05	4.53E-06	8.51E-05	9.456E-05	610	29		
GR 15-3	18	1882	1294	0.7104	-	-	0.164	0.411	13.945	0.1892	17.5	6.89E-05	5.35E-06	7.03E-05	8.308E-05	536	35		
GR 15.1 .1	14	773	284	0.3798	1.25E-02	6.10E+01	0.128	0.361	8.684	0.1591	8.5	7.53E-05	2.89E-06	7.66E-05	9.147E-05	590	19	570	29
GR 15.2 .1	8	2339	1922	0.8491	8.24E-03	3.20E+02	0.065	0.465	4.488	0.1054	13.0	7.73E-05	2.38E-06	7.82E-05	9.007E-05	581	15		
GR 15.3 .1	47	3366	146	0.4484	1.20E-01	2.08E+01	0.429	1.029	11.954	0.4148	14.8	6.05E-05	9.05E-06	6.48E-05	7.915E-05	510	58		
GR 15.4 .1	12	8383	380	0.4449	4.00E-02	3.90E+01	0.105	0.425	6.919	0.1396	8.2	7.66E-05	2.60E-06	7.77E-05	9.213E-05	594	17		
GR16																			
GR 16-1	9	2307	2146	0.9613	-	-	0.082	0.414	9.819	0.1198	14.6	7.46E-05	4.55E-06	7.55E-05	8.494E-05	548	29		
GR 16-2	8	7845	1811	2.3854	-	-	0.070	0.833	4.537	0.1092	6.4	8.60E-05	4.23E-06	8.69E-05	7.356E-05	474	27		

GR 16-3	6	3070	2767	0.9313	-	-	0.054	0.457	9.054	0.0962	17.4	6.96E-05	4.14E-06	7.03E-05	7.995E-05	515	27		
GR 16.1.1	15	22177	2024	0.9432	8.90E-03	1.10E+02	0.131	0.551	4.182	0.16111	8.1	8.26E-05	2.32E-06	8.40E-05	9.363E-05	604	15	550	21
GR 16.2.1	15	7001	266	0.3915	2.93E-02	1.10E+02	0.133	0.384	9.688	0.16344	11.0	7.19E-05	2.84E-06	7.32E-05	8.724E-05	562	18		
GR 16.3.1	21	4288	153	0.3687	4.36E-02	1.10E+02	0.193	0.607	10.810	0.21400	7.2	6.97E-05	2.56E-06	7.15E-05	8.568E-05	552	17		
GR 16.4.1	15	13599	782	0.5943	1.47E-02	1.10E+02	0.137	0.539	4.998	0.16663	8.2	8.30E-05	2.55E-06	8.45E-05	9.692E-05	625	16		
GR 16.1.6	23	9311	632	0.7011	3.03E-02	1.10E+02	0.206	0.606	9.307	0.22544	11.8	6.53E-05	3.39E-06	6.71E-05	7.859E-05	507	22		
GR 16.7.1	15	13322	1138	0.8827	2.05E-02	1.10E+02	0.136	0.579	5.617	0.16577	7.7	7.64E-05	2.27E-06	7.78E-05	8.784E-05	566	15		
GR 16.8.1	14	12922	942	0.7534	2.25E-02	1.10E+02	0.122	0.530	6.176	0.15341	10.0	7.22E-05	2.34E-06	7.34E-05	8.455E-05	545	15		
GR 16.9.1	18	11563	903	0.8067	2.33E-02	1.10E+02	0.165	0.583	9.185	0.19011	16.4	7.25E-05	4.24E-06	7.40E-05	8.472E-05	546	27		
GR24																			
GR 24-1	16	14098	820	0.6013	-	-	0.144	0.492	11.913	0.17222	23.4	7.69E-05	6.73E-06	7.84E-05	9.108E-05	587	43		
GR 24-2	29	23411	1854	0.8184	-7.90E-03	7.91E+00	0.263	0.808	7.921	0.27333	7.9	6.08E-05	4.37E-06	6.30E-05	7.398E-05	477	28	581	28
GR 24-3	7	22666	2069	0.9435	-	-	0.056	0.456	9.018	0.09978	13.8	9.29E-05	5.40E-06	9.38E-05	1.040E-04	671	35		
GR 24.1.1	13	6177	241	0.4037	4.38E-02	6.69E+01	0.112	0.378	15.050	0.14555	9.0	7.49E-05	2.41E-06	7.61E-05	9.026E-05	582	16		
GR 24.2.1	11	16122	1020	0.6541	1.99E-02	5.09E+01	0.099	0.440	7.826	0.13455	11.8	7.76E-05	2.41E-06	7.87E-05	9.106E-05	587	16		

Table 3. SHRIMP zircon U–Pb analytical results (< 2 Ma) obtained at the Australian National University SHRIMP center.

					Total Pb, before common Pb correction										Corrected for disequilibrium			Mean	
	Pb	U	Th		204Pb			208Pb		207Pb		206Pb		206Pb*	and initial 234U and 230Th			sample	95%
Sample	ppb	ppm	ppm	Th/U	206Pb	±	f206(%)	206Pb	±	206Pb	±	238U	±	238U	206Pb*/ 238U	Date (ka)	±	age (ka)	c.l.
GR5																			
5B-1.1	42	1488	869	0.58	-	-	0.069	0.354	0.058	0.11966	0.01299	2.85E-05	8.6E-07	2.66E-05	3.96E-05	255	6		
5B-2.1	80	2910	4434	1.52	-	-	0.001	0.599	0.037	0.05800	0.00700	2.74E-05	6.3E-07	2.74E-05	3.68E-05	237	4		
5B-3.1	20	769	440	0.57	3.94E-03	3.75E-03	0.089	0.431	0.103	0.13755	0.02033	2.62E-05	1.4E-06	2.38E-05	3.66E-05	236	9		
5B-4.1	39	1595	1140	0.71	2.05E-02	6.36E-03	0.069	0.448	0.043	0.11999	0.02077	2.45E-05	7.8E-07	2.28E-05	3.49E-05	225	5		
5B-5.1	31	1229	894	0.73	3.99E-02	1.28E-02	0.078	0.403	0.047	0.12755	0.02911	2.56E-05	1.1E-06	2.36E-05	3.57E-05	230	7		
5B-6.1	51	2042	1499	0.73	4.63E-03	2.62E-03	0.086	0.460	0.044	0.13444	0.01888	2.49E-05	6.8E-07	2.27E-05	3.47E-05	224	4		
5B-9.1	43	1758	1252	0.71	-	-	0.120	0.394	0.046	0.16658	0.02177	2.47E-05	8.9E-07	2.17E-05	3.37E-05	217	6		
5B-11.1	26	1119	712	0.64	-	-	0.070	0.395	0.056	0.12055	0.02222	2.36E-05	1.7E-06	2.19E-05	3.41E-05	220	11		
5B-12.1	27	1070	658	0.62	1.71E-02	6.16E-03	0.092	0.438	0.057	0.14055	0.01711	2.56E-05	1.1E-06	2.32E-05	3.57E-05	230	7		
5B-13.1	62	2123	1914	0.90	-	-	0.054	0.453	0.037	0.10558	0.01311	2.92E-05	1.2E-06	2.76E-05	3.95E-05	255	7		
5B-14.1	28	992	750	0.76	1.20E-02	4.73E-03	0.073	0.562	0.122	0.12231	0.02133	2.77E-05	1.1E-06	2.57E-05	3.79E-05	245	7	230	4
5B-15.1	35	1248	977	0.78	4.86E-03	4.36E-03	0.070	0.387	0.069	0.12000	0.01666	2.79E-05	1.3E-06	2.60E-05	3.81E-05	246	8		
GR5-1.1	23	974	537	0.55	1.76E-02	1.00E-02	0.113	0.450	0.084	0.15955	0.02433	2.36E-05	1.5E-06	2.09E-05	3.33E-05	215	10		
GR5-2.1	13	484	221	0.46	3.30E-03	1.57E-03	0.171	0.502	0.089	0.21119	0.04433	2.68E-05	1.7E-06	2.22E-05	3.52E-05	227	11		
GR5-3.1	16	566	305	0.54	4.93E-02	2.70E-02	0.161	0.543	0.133	0.20255	0.04477	2.86E-05	1.9E-06	2.40E-05	3.69E-05	238	12		
GR5-4.1	18	661	317	0.48	6.37E-02	1.84E-02	0.126	0.520	0.099	0.17122	0.02811	2.72E-05	2.1E-06	2.38E-05	3.71E-05	239	13		
GR5-	19	79	35	0.4	4.10E-	1.58E-	0.117	0.563	0.11	0.1162	0.0231	2.41E-	2.5E-	2.13E-	3.42E-05	220	16		

7.1		3	9	5	02	02			1	9	5	05	06	05				
GR5-11.1	39	1594	8088	0.51	2.37E-02	1.08E-02	0.075	0.334	0.0051	0.1248	0.0187	2.43E-05	9.4E-07	2.24E-05	3.53E-05	227	6	
GR5-12.1	18	6873	3007	0.45	-	-	0.171	0.439	0.0955	0.2120	0.0370	2.59E-05	2.3E-06	2.14E-05	3.44E-05	221	15	
GR5-13.1	41	1436	1017	0.71	1.45E-02	7.49E-03	0.079	0.433	0.0049	0.1282	0.0159	2.83E-05	1.5E-06	2.61E-05	3.85E-05	248	10	
GR5-14.1	35	1323	8442	0.64	8.41E-03	5.73E-03	0.097	0.423	0.0073	0.1450	0.0184	2.61E-05	9.4E-07	2.35E-05	3.60E-05	232	6	
GR5-15.1	23	9705	5475	0.56	-	-	0.113	0.462	0.0139	0.1593	0.0248	2.42E-05	1.3E-06	2.14E-05	3.39E-05	219	8	
GR5-16.1	32	1287	9255	0.72	2.22E-02	7.18E-03	0.088	0.521	0.0059	0.1370	0.0208	2.45E-05	1.2E-06	2.24E-05	3.43E-05	221	8	
GR12																		
12-1.1	255	1729	1391	0.80	-	-	0.004	0.285	0.0017	0.0520	0.0048	1.47E-04	3.4E-06	1.47E-04	1.61E-04	1036	21	
12-2.1	69	4559	1554	0.34	6.60E-04	3.88E-04	0.020	0.206	0.0023	0.0661	0.0136	1.50E-04	6.5E-06	1.47E-04	1.62E-04	1046	42	
12-4.1	230	1577	1546	0.98	-	-	0.004	0.344	0.0015	0.0517	0.0052	1.46E-04	1.9E-06	1.45E-04	1.59E-04	1023	12	
12-5.1	206	1486	7775	0.52	1.56E-03	7.49E-04	0.015	0.200	0.0012	0.0620	0.0040	1.39E-04	1.8E-06	1.36E-04	1.51E-04	977	12	
12-6.1	811	5519	1976	0.36	4.14E-03	3.06E-03	0.015	0.173	0.0032	0.0618	0.0110	1.46E-04	3.3E-06	1.44E-04	1.60E-04	1029	21	1023	18
12-7.1	71	4799	2696	0.56	2.23E-03	3.02E-03	0.016	0.267	0.0024	0.0628	0.0068	1.49E-04	3.9E-06	1.46E-04	1.61E-04	1039	25	
12-9.1	151	1062	7367	0.69	-	-	0.017	0.264	0.0024	0.0631	0.0054	1.42E-04	2.5E-06	1.40E-04	1.54E-04	993	16	
12-10.1	98	6800	2883	0.42	1.54E-03	1.08E-03	0.014	0.190	0.0027	0.0611	0.0061	1.45E-04	5.6E-06	1.43E-04	1.58E-04	1020	36	
12-11.1	42	2733	1063	0.39	1.31E-02	5.83E-03	0.041	0.186	0.0040	0.0857	0.0200	1.55E-04	4.9E-06	1.49E-04	1.65E-04	1062	31	
GR14																		
14-1.1	91	1192	8300	0.70	-	-	0.024	0.269	0.0040	0.0718	0.0109	7.67E-05	2.0E-06	7.48E-05	8.92E-05	575	13	
14-1.2	177	1764	1589	0.90	1.06E-02	3.70E-03	0.122	0.577	0.0042	0.1608	0.0111	1.00E-04	7.3E-06	8.80E-05	1.01E-04	654	47	
14-2.1	48	5942	2855	0.48	1.15E-02	3.91E-03	0.048	0.217	0.0029	0.0942	0.0105	8.11E-05	2.5E-06	7.72E-05	9.27E-05	598	16	582	20
14-3.1	115	1461	9344	0.64	5.59E-03	3.66E-03	0.031	0.273	0.0024	0.0785	0.0065	7.88E-05	2.6E-06	7.63E-05	9.10E-05	586	17	
	1	1	1	0.	2.83	1.34	0.0	0.2	0.	0.0	0.0	7.81	1.4	7.56	8.99E	57	9	

14-4.1	17	4998	0873	E-03	E-03	32	80	0270	7905	E-05	E-06	E-05	-05	9			
GR16																		
16-1.1	227	24173	23544	0.97	6.41E-03	1.49E-03	0.139	0.618	0.0266	0.17633	0.01355	9.40E-05	2.4E-06	8.10E-05	9.42E-05	607	15	
16-4.1	110	14422	9722	0.67	6.99E-04	2.61E-04	0.030	0.296	0.033	0.07669	0.00062	7.60E-05	1.9E-06	7.38E-05	8.83E-05	569	12	
16-6.1	165	21258	16288	0.77	6.17E-04	3.78E-04	0.022	0.285	0.020	0.07001	0.00049	7.78E-05	1.1E-06	7.61E-05	9.02E-05	581	7	581	14
16-7.1	93	11728	8190	0.70	1.28E-03	9.05E-04	0.008	0.280	0.037	0.00572	0.00999	7.95E-05	2.4E-06	7.89E-05	9.32E-05	601	16	
16-9.1	177	22604	24422	1.08	5.88E-04	3.40E-04	0.029	0.409	0.019	0.07688	0.00072	7.82E-05	1.3E-06	7.59E-05	8.87E-05	572	9	
GR24																		
24-1.1	46	6241	2211	0.35	-	-	0.035	0.174	0.0244	0.00821	0.00128	7.35E-05	3.3E-06	7.09E-05	8.69E-05	560	21	
24-1.2	58	7233	34407	0.47	2.98E-03	1.87E-03	0.021	0.217	0.0266	0.00691	0.00124	8.03E-05	2.2E-06	7.86E-05	9.39E-05	606	14	
24-2.1	161	20388	15566	0.76	2.11E-03	1.16E-03	0.028	0.297	0.017	0.00758	0.00052	7.90E-05	1.2E-06	7.67E-05	9.09E-05	586	8	591	16
24-1.3	49	59823	23038	0.38	2.16E-03	1.86E-03	0.036	0.134	0.021	0.00829	0.00102	8.22E-05	2.4E-06	7.93E-05	9.50E-05	612	16	
24-1.4	50	63825	32551	0.51	2.98E-03	1.82E-03	0.037	0.206	0.033	0.00837	0.00097	7.87E-05	2.2E-06	7.58E-05	9.10E-05	587	14	

Table 4. U-Pb data for LA-ICP-MS analysis of zircons from Grenada, Carriacou and Petite Martinique islands
(measured in the Natural History Museum, London and Mainz University). In bold best ages.

													Age (Ma)					
Sample	U in ppm	Th in ppm	Th/U	207Pb/235U	±	206Pb/238U	±	rho	207Pb/206Pb	±	208Pb/232Th	±	207Pb/235U	±	206Pb/238U	±	207Pb/206Pb	±
ICP-MS-London																		
GR30																		
GR30-02	116	86	0.74	28.7649	0.7817	0.7076	0.0214	0.58	0.2998	0.0080	0.2018	0.0460	3446	27	3449	81	**3469**	**41**
GR30-05	364	295	0.81	26.2528	1.1680	0.6574	0.0304	0.82	0.2946	0.0080	0.1889	0.0622	3356	44	3257	119	**3442**	**42**
GR42																		
GR42-01	261	66	0.25	0.0147	0.0031	0.0025	0.0003	0.14	0.0496	0.0112	0.0010	0.1687	14.8	3.1	**15.8**	**1.8**	176	527
GR42-02	362	99	0.27	0.0155	0.0019	0.0023	0.0001	0.08	0.0522	0.0069	0.0010	0.1312	15.6	1.9	**15.0**	**0.9**	294	303
GR42-03	431	142	0.33	0.0150	0.0025	0.0025	0.0001	0.22	0.0478	0.0077	0.0008	0.1551	15.1	2.5	**15.8**	**0.9**	89	383
GR42-04	159	47	0.29	2.7137	0.0755	0.2272	0.0060	0.51	0.0882	0.0024	0.0722	0.0952	1332	21	1320	32	**1387**	52
GR42-05	221	58	0.26	2.0315	0.0463	0.1910	0.0039	0.55	0.0783	0.0016	0.0643	0.1223	1126	16	1127	21	**1155**	41
GR42-06	488	149	0.30	0.0169	0.0023	0.0025	0.0001	0.23	0.0524	0.0071	0.0009	0.1032	17.0	2.3	**15.8**	**0.9**	303	310
GR42-07	141	93	0.66	2.7468	0.0712	0.2336	0.0061	0.54	0.0869	0.0022	0.0712	0.0513	1341	19	1353	32	**1358**	**48**
GR42-08	105	61	0.58	2.7706	0.0713	0.2303	0.0052	0.45	0.0888	0.0023	0.0690	0.0615	1348	19	1336	28	**1400**	**49**
GR42-11	286	64	0.22	11.909	0.3023	0.4734	0.0122	0.60	0.1843	0.0042	0.0816	0.2739	2597	24	2499	54	**2692**	**38**
GR45																		
GR45-01	461	102	0.22	0.0324	0.0018	0.0053	0.0001	0.03	0.0462	0.0028	0.0017	0.1219	32.3	1.8	**34.3**	**0.9**	8	-148
GR45-03	542	127	0.24	0.0353	0.0021	0.0053	0.0001	0.10	0.0505	0.0031	0.0018	0.1257	35.3	2.0	**34.3**	**0.9**	218	144
GR45-05	280	64	0.23	0.0347	0.0037	0.0052	0.0003	0.12	0.0523	0.0059	0.0018	0.2223	34.6	3.6	**33.4**	**1.8**	299	258
ICP-MS-Mainz																		
GR45																		
GR45-1	1622	284	0.17	0.0286	0.0022	0.0045	0.0002	0.22	0.0475	0.0038	0.0017	0.1452	28.6	2.2	**28.8**	**1.2**	74	188
GR45-2	2433	534	0.22	0.0286	0.0020	0.0042	0.0002	0.20	0.0506	0.0038	0.0014	0.1045	28.6	2.0	**26.9**	**1.1**	223	174
GR45-3	748	95	0.13	0.0311	0.0043	0.0045	0.0002	0.22	0.0503	0.0069	0.0017	0.2519	31.1	4.2	**28.8**	**1.6**	209	316
GR45-4	582	146	0.2	0.2833	0.018	0.0349	0.001	0.4	0.0592	0.003	0.0139	0.601	253.3	14.	**221.1**	**9.**	574	12

			5		0		5	7		4		9		3		**0**		4
			0.		0.0		0.0	0.		0.0		0.1				**1**		2
GR4			2	0.031	03	0.004	00	1	0.051	05	0.001	36	31.	3.	**29.**	**.**	25	4
5-5	968	237	4	4	2	6	2	4	3	4	7	6	4	2	**4**	**2**	4	3
			0.		0.0		0.0	0.		0.0		0.1				**1**		3
GR4			2	0.027	03	0.004	00	2	0.046	06	0.001	40	27.	3.	**28.**	**.**		2
5-6	634	162	6	0	6	4	2	0	1	1	5	8	0	5	**1**	**6**	3	1
			~~0.~~		~~0.0~~		~~0.0~~	~~0.~~		~~0.0~~		~~0.0~~				~~1~~		~~1~~
~~GR4~~	~~356~~	~~116~~	~~3~~	~~0.057~~	~~05~~	~~0.005~~	~~00~~	~~5~~	~~0.083~~	~~06~~	~~0.003~~	~~84~~	~~56.~~	~~5.~~	~~31.~~	~~.~~	~~12~~	~~6~~
~~5-7~~	~~2~~	~~4~~	~~3~~	~~7~~	~~9~~	~~0~~	~~3~~	~~8~~	~~2~~	~~9~~	~~2~~	~~6~~	~~9~~	~~7~~	~~9~~	~~7~~	~~74~~	~~3~~
			0.		0.0		0.0	0.		0.0		0.1				**1**		3
GR4			1	0.030	03	0.004	00	1	0.050	06	0.001	97	30.	3.	**28.**	**.**	19	1
5-8	782	138	8	1	9	5	2	4	0	7	9	4	1	8	**8**	**6**	5	0
			0.		0.0		0.0	0.		0.0		0.2		1		**9**		1
GR4			1	0.240	13	0.034	01	3	0.051	02	0.012	81	21	1.	**21**	**.**	24	3
5-9	429	49	1	6	8	6	5	9	1	9	6	6	8.9	4	**9.3**	**3**	5	1
			0.		0.0		0.0	0.		0.0		0.0				**1**		2
GR4			2	0.034	03	0.004	00	1	0.055	06	0.001	94	34.	3.	**30.**	**.**	42	4
5-11	875	234	7	6	6	7	2	0	3	0	6	2	5	6	**0**	**2**	4	3
			0.		0.0		0.0	0.		0.0		0.0				**1**		3
GR4			3	0.036	04	0.005	00	1	0.049	06	0.001	79	36.	4.	**34.**	**.**	18	0
5-12	532	165	1	3	8	3	3	8	7	6	9	3	2	7	**4**	**7**	1	8
			0.		0.0		0.0	0.		0.0		0.1				**1**		2
GR4			2	0.042	04	0.004	00	2	0.067	07	0.002	15	42.	4.	**30.**	**.**	85	2
5-14	685	201	9	8	7	7	2	5	4	3	2	2	6	6	**0**	**2**	0	4
			0.		0.0		0.0	0.		0.0		0.1				**1**		1
GR4	154		2	0.032	02	0.004	00	2	0.052	04	0.001	34	32.	2.	**29.**	**.**	31	7
5-15	1	341	2	4	4	6	2	0	6	1	8	2	3	4	**4**	**2**	2	7
			0.		0.0		0.0	0.		0.0		0.0				**1**		1
GR4	217		2	0.030	02	0.004	00	3	0.047	03	0.001	87	30.	2.	**30.**	**.**		6
5-16	2	573	6	1	1	7	2	1	3	2	6	0	1	0	**0**	**2**	64	2
			0.		0.0		0.0	0.		0.0		0.1				**1**		2
GR4			1	0.038	05	0.004	00	2	0.059	07	0.002	83	38.	5.	**31.**	**.**	57	8
5-17	489	72	5	9	2	9	3	2	3	8	1	9	8	1	**3**	**7**	8	6
PM2b																		
			1.		0.0		0.0	0.		0.0		0.0				**0**		1
PM2	165	225	3	0.014	00	0.002	00	1	0.049	02	0.000	16	14.	0.	**14.**	**.**	16	3
b-01	2	0	6	4	8	2	0	0	4	8	7	8	5	8	**1**	**1**	7	4
			0.		0.0		0.0	0.		0.0		0.0				**0**		1
PM2	158	128	8	0.015	00	0.002	00	1	0.054	02	0.000	26	15.	0.	**14.**	**.**	38	2
b-02	0	4	1	2	8	2	0	3	3	9	8	1	3	8	**1**	**1**	4	2
PM2			0.		0.0		0.0	0.		0.0		0.0				**0**		2
b-03.1	135	114	8	0.014	01	0.002	00	3	0.051	04	0.000	36	14.	1.	**14.**	**.**	25	0
	4	3	4	8	2	2	1	0	3	5	7	8	9	2	**1**	**9**	4	3
PM2			0.		0.0		0.0	0.		0.0		0.0				**0**		1
b-03.2	135	114	8	0.015	01	0.002	00	3	0.052	04	0.000	35	15.	1.	**14.**	**.**	32	9
	4	4	4	2	2	2	1	1	8	5	7	9	3	2	**1**	**9**	0	5
			0.		0.0		0.0	0.		0.0		#DI				**0**		2
PM2			8	0.014	01	0.002	00	2	0.055	05	0.000	V/0	14.	1.	**13.**	**.**	41	2
b-04	698	605	7	5	4	0	1	3	1	6	0	!	7	4	**2**	**9**	6	8
			0.		0.0		0.0	0.		0.0		0.0				**0**		3
PM2			5	0.014	01	0.002	00	0	0.057	08	0.000	64	14.	1.	**13.**	**.**	51	1
b-07	459	253	5	4	9	0	1	7	6	3	7	4	5	9	**2**	**9**	5	7

Highlights

- Presence of late Jurassic to Paleoarchean (158–3469 Ma) xenocrysts within volcanic rocks and beach and river sands of the southern Lesser Antilles.
- Evidence for the assimilation of detrital sediments from the intra-arc proto-Grenada/Tobago basin.
- The xenocrystic zircons could have been derived from the Eastern Andean Cordillera of Colombia, the Merida Andes, and the northern Venezuela coastal ranges.
- A new analytical procedure was developed to correct for lack of secular equilibrium in the ^{238}U decay chain.